3.2.3
6.29

NAA-SR-8906
COPY

MASTER

HEAT TRANSFER AND VOID FORMATION DURING FORCED CIRCULATION BOILING OF ORGANIC COOLANTS

AEC Research and Development Report

ATOMICS INTERNATIONAL
A DIVISION OF NORTH AMERICAN AVIATION, INC.

DISCLAIMER

This report was prepared as an account of work sponsored by an agency of the United States Government. Neither the United States Government nor any agency thereof, nor any of their employees, makes any warranty, express or implied, or assumes any legal liability or responsibility for the accuracy, completeness, or usefulness of any information, apparatus, product, or process disclosed, or represents that its use would not infringe privately owned rights. Reference herein to any specific commercial product, process, or service by trade name, trademark, manufacturer, or otherwise does not necessarily constitute or imply its endorsement, recommendation, or favoring by the United States Government or any agency thereof. The views and opinions of authors expressed herein do not necessarily state or reflect those of the United States Government or any agency thereof.

DISCLAIMER

Portions of this document may be illegible in electronic image products. Images are produced from the best available original document.

LEGAL NOTICE

This report was prepared as an account of Government sponsored work. Neither the United States, nor the Commission, nor any person acting on behalf of the Commission:

A. Makes any warranty or representation, express or implied, with respect to the accuracy, completeness, or usefulness of the information contained in this report, or that the use of any information, apparatus, method, or process disclosed in this report may not infringe privately owned rights; or

B. Assumes any liabilities with respect to the use of, or for damages resulting from the use of information, apparatus, method, or process disclosed in this report.

As used in the above, "person acting on behalf of the Commission" includes any employee or contractor of the Commission, or employee of such contractor, to the extent that such employee or contractor of the Commission, or employee of such contractor prepares, disseminates, or provides access to, any information pursuant to his employment or contract with the Commission, or his employment with such contractor.

Price $1.50
Available from the Office of Technical Services
Department of Commerce
Washington 25, D. C.

NAA-SR-8906
REACTOR TECHNOLOGY
57 PAGES

HEAT TRANSFER AND VOID FORMATION DURING FORCED CIRCULATION BOILING OF ORGANIC COOLANTS

By
F. BERGONZOLI
F. J. HALFEN

ATOMICS INTERNATIONAL
A DIVISION OF NORTH AMERICAN AVIATION, INC.
P.O. BOX 309 CANOGA PARK, CALIFORNIA

CONTRACT: AT(11-1)-GEN-8
ISSUED: JUN 15 1964

DISTRIBUTION

This report has been distributed according to the category "Reactor Technology" as given in "Standard Distribution Lists for Unclassified Scientific and Technical Reports" TID-4500 (27th Ed.), February 1, 1964. A total of 711 copies was printed.

ACKNOWLEDGMENT

The authors would like to acknowledge the cooperation and assistance of W. H. Wickes and A. F. Lillie who conducted the experimental program. The authors are also indebted to A. A. Jarrett who provided invaluable assistance and guidance during the program.

ABSTRACT

The experimental results of an extensive parameter survey are reported for forced circulation boiling of organic coolants.

The observed effect of dissolved gas on the onset of nucleate boiling and on the overall heat transfer behavior of boiling organic coolants is discussed. The boiling heat transfer and void fraction results for degassed coolants are correlated by existing models or modifications of existing models whenever possible. A new model is presented for the correlation of the void fraction data at or near saturation conditions. The possibility of application of this model to other systems and geometries is explored. The effect of system pressure and quality on the slip ratio of organic coolant vapor is illustrated.

The tests were conducted in a closed circulation loop at low system pressures (1 to 2 atmospheres). A d.c. resistance heated test section consisting of a vertical, seamless nickel tube of 9/16 in. O.D. with a 0.042 in. wall thickness and having a heated length of 12 ft was used in these experiments.

CONTENTS

TABLES

TABLES

FIGURES

I. INTRODUCTION

An area of major concern in hazards evaluations of organic-cooled reactors is the accurate representation of a loss-of-pressure accident resulting in boiling of the coolant in the reactor core.[1] An analytical model describing this type accident basically requires correlations for forced circulation boiling heat transfer, void formation, and two-phase flow. Over the past years, the development and application of correlations of this nature has centered mainly on boiling water systems. This particular emphasis has been recently accentuated by the technological requirements of boiling water reactors. Consequently, available correlations are either specific to water systems, or, if generalized, require experimental verification of their applicability to other systems. This is particularly the case for typical organic coolants which, rather than being single components, are a mixture of various components. For instance, Santowax-R normally used as the coolant in organic-moderated reactors is a mixture of terphenyl isomers with varying small percentages of diphenyl and other organic compounds. Irradiated Santowax-R will contain pyrolytic and radiolytic decomposition products in addition to its basic constituents. It is therefore the intent of the experimental surveys here reported to determine either the validity of existing generalized correlations[2] in describing the steady-state boiling behavior of organic coolants or, if required, to develop correlations which will satisfactorily describe this behavior. The ultimate objective of either case is to obtain a solid basis from which to develop the more sophisticated pressure transient models[3] required for the analysis of loss-of-pressure accidents. In the light of the ultimate objectives, this experimental effort has been concentrated on the investigation of the basic parameters influencing boiling heat transfer and void formation at representative operating ranges of pressure and temperature. The geometry and flow orientation of the system are comparable to those encountered in organic-cooled nuclear reactors.

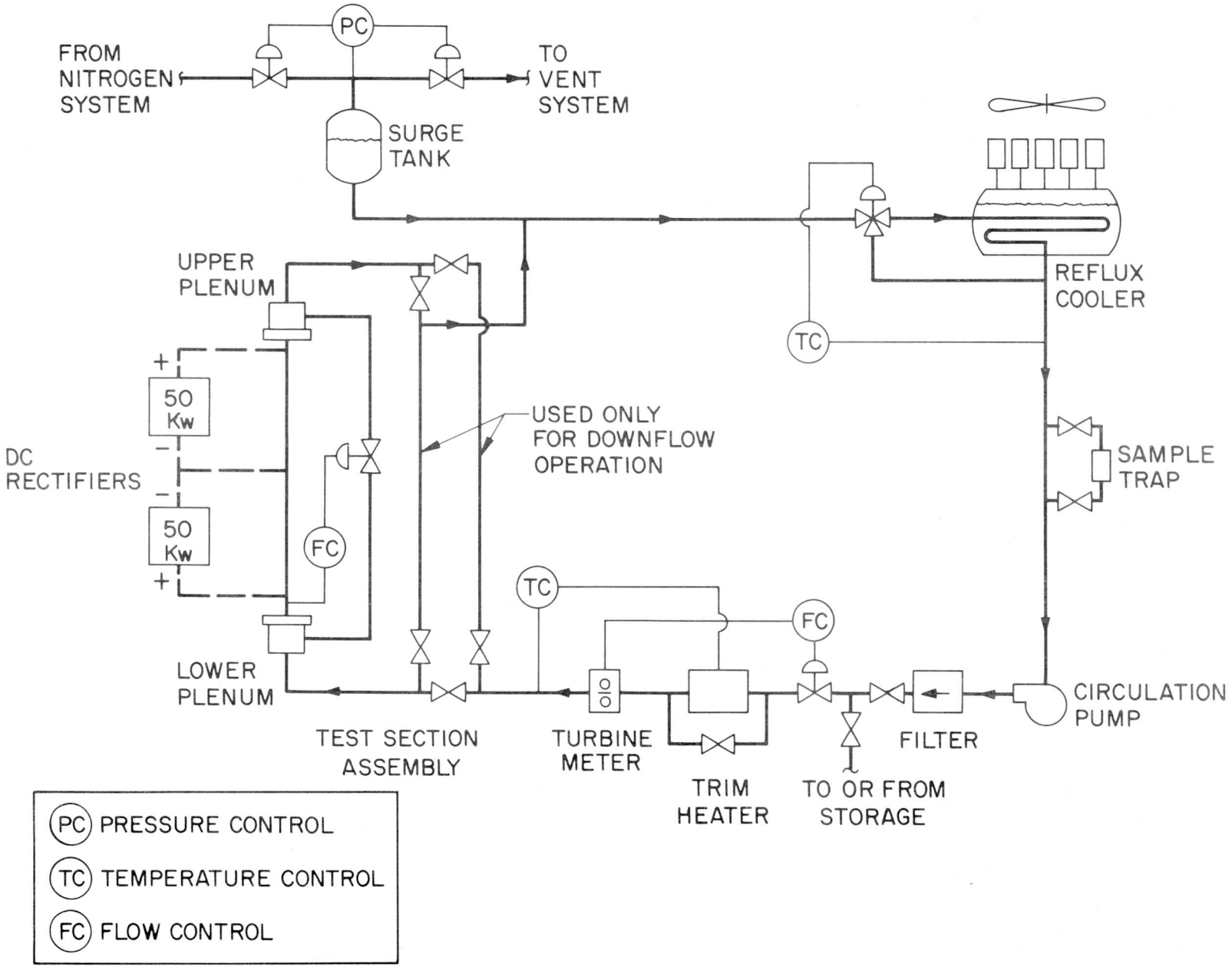

Figure 1. Flow Stability Test Loop

II. EXPERIMENTAL FACILITIES

The experimental facilities consist essentially of a closed loop wherein the circulating coolant undergoes a heating and cooling cycle at controlled conditions of flow, temperature, and pressure. The test loop is pressurized with nitrogen in the surge tank. A schematic of the test loop is presented in Figure 1. A detailed description of the experimental facilities and related instrumentation is presented in Reference 4.

A. TEST SECTION

The test section (see Figure 2) consists of a seamless nickel tube 9/16 in. O. D. with a 0.042 in. wall thickness of close tolerance. It is electrically heated with d. c. power by means of power terminals connected directly to the test section. The heated length is 12 ft and the total tube length is 13 ft. The test section has a vertical orientation and the loop piping arrangement provides for either upflow or downflow circulation of the coolant.

B. BASIC INSTRUMENTATION

The instrumentation provided for the test section measures and records the following test data:

1) Void fraction,

2) Coolant and wall temperatures,

3) System pressure and pressure drops,

4) Coolant flowrate, and

5) Power input.

The instrumentation is suitable for both the steady-state and the transient phases of the experimental program. The measured variables are recorded by a multichannel direct recording oscillograph on an 8-in. wide chart.

1. Void Fraction Measurement

The volume fraction of the organic coolant vapor at any preselected point along the test section is measured by a system consisting of a 150-kw x-ray machine, collimators, and two detectors. The x-ray beam is split and

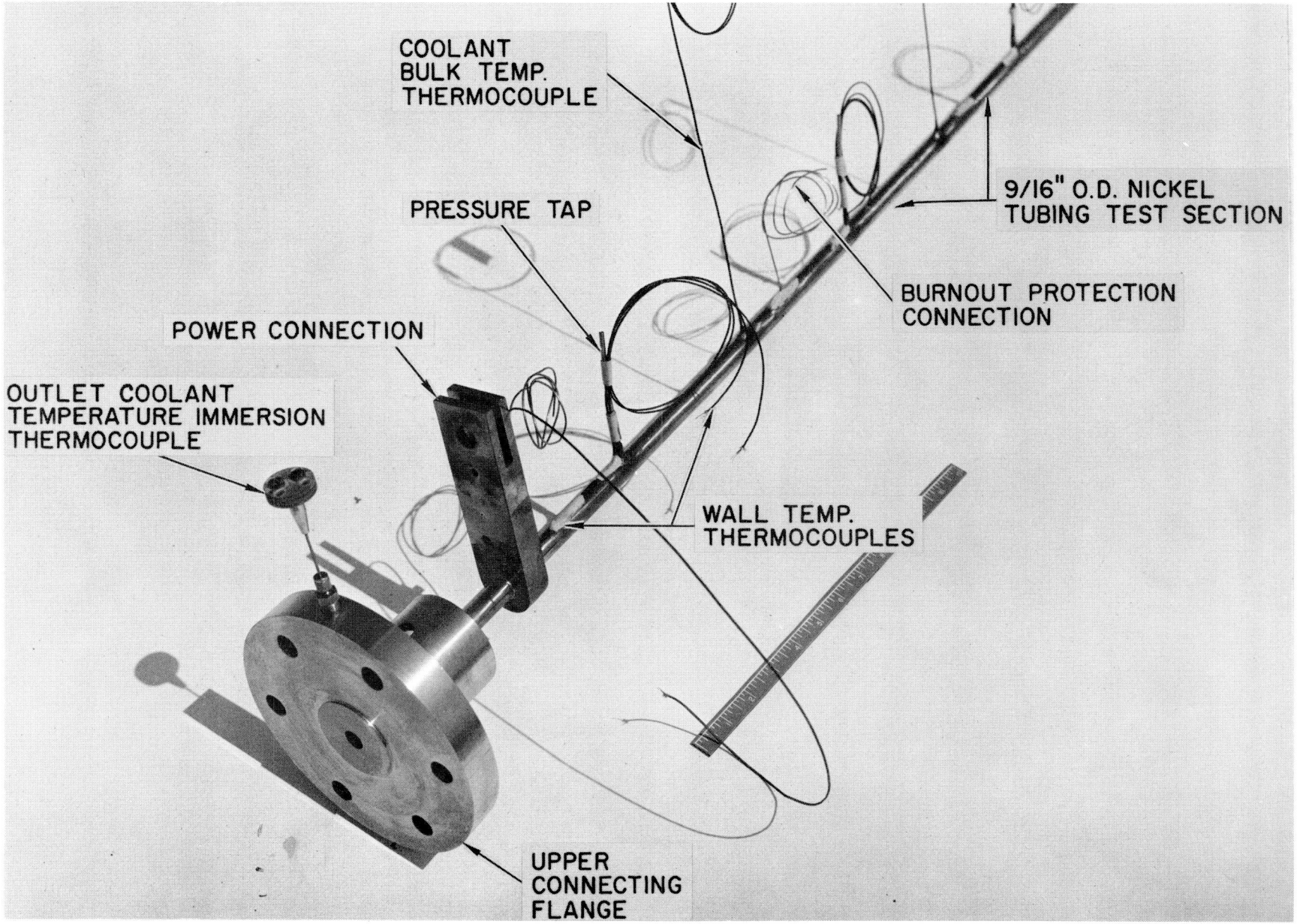

Figure 2. Test Section of Loop

collimated into two beams. One beam is transmitted through a "dummy" test section, through another collimator, and into a scintillation detector. The other beam is collimated in like manner, and passes through the test section to another collimated detector. The output of each detector goes into a differential amplifier which subtracts the reference detector signal from the void detector signal. The output signal from the differential amplifier drives a high speed galvanometer, calibrated in "void fraction." A complete description of the void fraction measuring system, including system calibration and accuracy, is reported in Reference 5.

2. Temperature Measurements

Chromel-constantan thermocouples are used for measurement of coolant and wall temperatures. Thermocouples which measure test-section wall temperatures are attached to the wall with pure silver to minimize the voltage pickup from the d. c. -heated tube. Thermocouples which measure coolant bulk temperatures are inserted directly in to the coolant stream and are insulated from the test section wall. Coolant and wall thermocouples are located along the length of the test section at representative intervals to provide comprehensive temperature profiles for heat transfer analysis.

3. Pressure Measurements

Absolute and differential pressures are measured with variable reluctance transducers. These transducers consist of a pressure sensing diaphragm of magnetic material, the deflection of which controls a gap in each of two magnetic circuits. The gaps change in opposite directions and produce corresponding changes in the inductance of two pick-off coils. This effect is utilized in an a. c. bridge circuit to produce an output voltage proportional to the applied pressure.

Absolute pressures are measured at the inlet and outlet of the test section. Differential pressures are measured at incremental points along the test section to provide a representative pressure profile of the system.

4. Other Measurements

Two means of measuring coolant flowrate for steady-state tests are available. The first is a turbine flowmeter which measures total test loop flowrate. The second is the test section inlet differential pressure transducer which is calibrated in terms of flowrate.

Power inputs to the test section, from which the heat flux is determined, is measured by recording wattmeters. The voltage and current of the test section are indicated on high-precision voltmeters and ammeters.

C. EXPERIMENTAL METHOD

The tests covered in this investigation were conducted at preselected and constant conditions of system pressure, flow rate, heat flux, and coolant inlet temperature. Selection of the specific operating conditions for a given test was made to determine the relative effects of individual variables on the boiling behavior of the coolant investigated. This parameter study was performed over a representative range of subcooled and saturated-coolant conditions. The ranges considered for the variables investigated are typical for analysis of loss-of-pressure accidents. A description of the operating and control procedure followed in these experiments is presented in Reference 4.

III. RESULTS

Forced circulation nucleate boiling experiments were conducted with two organic fluids, isopropyl diphenyl and Santowax-R. The tests with isopropyl diphenyl were limited to an investigation of the boiling heat transfer behavior of the coolant flowing upwards in the vertical test section. The tests with Santowax-R, in addition to heat transfer data, included measurements of void fraction with both upflow and downflow circulation of the coolant through the test section.

Tabulation of all results is presented in the Appendix A (Tables A-1 to A-5), and a summary of the coolant physical properties over the pressure and temperature ranges investigated is given in Appendix B (Table B-1). The ranges for the variables investigated are as follows:

Heat Flux: 27,000 to 110,000 Btu/hr-ft^2

Inlet Coolant Velocity: 5 to 14 ft/sec

System Pressure: 15 to 35 psia

A. BOILING HEAT TRANSFER

1. Isopropyl Diphenyl

The experiments consistently indicated the existence of two subcooled boiling zones within the 12-ft long test section (see Figure 3). The first zone is a premature subcooled boiling zone caused by the lowering of the saturation temperature of the coolant by the presence of dissolved nitrogen (the loop is pressurized by nitrogen gas in the surge tank). The second zone is a normal organic subcooled boiling zone, apparently not affected by nitrogen. The transition from the first to the second zone indicates that, as boiling progresses, the effective saturation temperature of the coolant increases to its normal value. The nitrogen liberated during the boiling process does not quickly redissolve. Since this progressively reduces the dissolved nitrogen concentration along the test section, the effective saturation temperature approaches that for the degassed coolant.

Correlation of the heat transfer data for the first zone was not feasible due to the uncertainties related to the effective saturation temperature of the

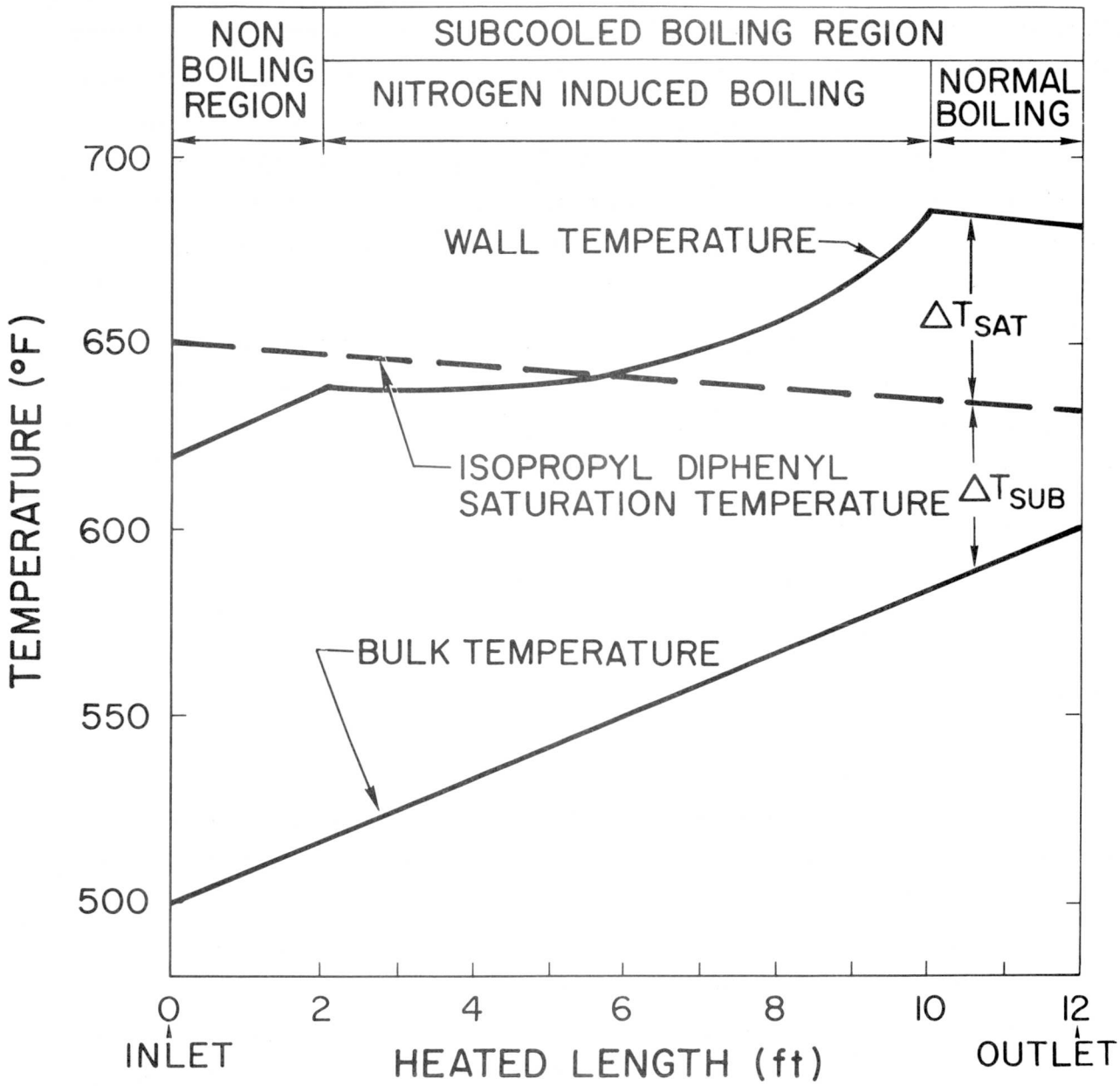

Figure 3. Effect of Dissolved Nitrogen on the Subcooled Boiling of Isopropyl Diphenyl

coolant containing dissolved nitrogen. The boiling heat transfer data for the second zone (Table A-1) were correlated satisfactorily by use of Levy's boiling heat transfer equation.[6] A correlation constant, $1/B_L$, was determined as a function of pressure and is shown in Figure 4. The correlation of the data for isopropyl diphenyl is shown in Figure 5. The data lie within ±10% of the correlation line. These data were not correlated with other equations because of the uncertainty in the property value for the surface tension and its variation with temperature.

2. Santowax-R

During these experiments, an effort was made to minimize the dissolved nitrogen concentration in the coolant. The coolant in the surge tank was kept slightly above the freezing point at which temperature the gas solubility is low. The low operating pressure at which the experiments were conducted also helped to lower the solubility of nitrogen in the coolant. Consequently, the extended nitrogen induced boiling zone, observed in the case of isopropyl diphenyl, was considerably reduced and in most instances practically eliminated.

Forced circulation boiling heat transfer data for Santowax-R have been correlated (Table A-2) with equations of Levy,[6] Rohsenow,[7] and Forster-Greif.[8] An experimental correlation constant, $1/B_L$, was determined as a function of pressure for Levy's equation as shown in Figure 4. By use of this correlation constant, data are correlated within ±10% by Levy's equation as shown in Figure 6. Correlation of the data with Rohsenow's equation is shown in Figure 7. Most of the data lie within ±10% of the correlation line. This equation uses a correlation constant independent of pressure.

The Forster-Greif Correlation-I was used in an attempt to correlate the data as shown in Figure 8. This resulted in a poor correlation since much of the data is outside ±25% of the correlation line. The Forster-Greif Correlation-II was not used because a discrepancy was found in the units used in the equation as given in Reference 8.

Upflow and downflow boiling heat transfer experiments were conducted with Santowax-R. There was no noticeable difference between the upflow and downflow results; both are included in the tables and illustrations.

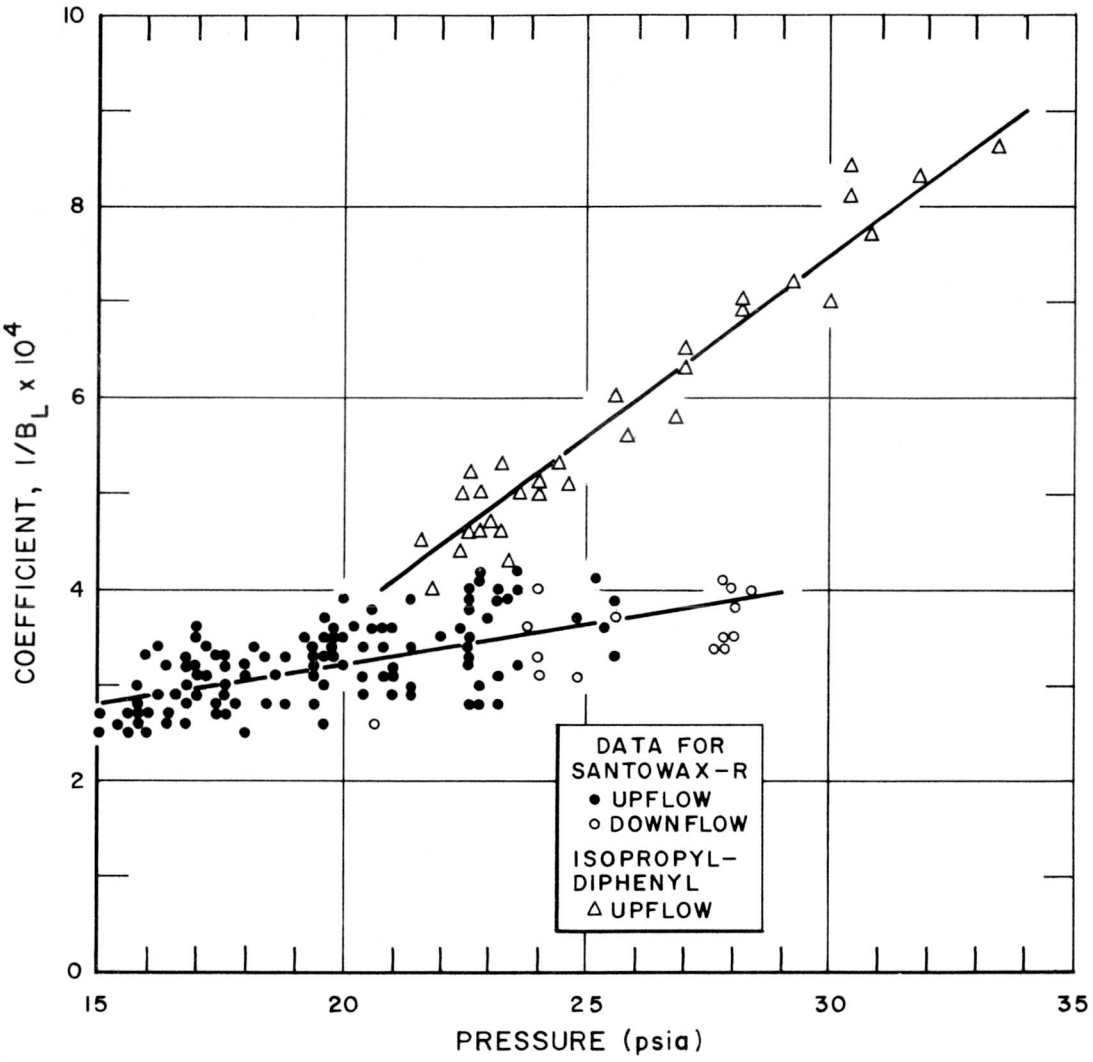

Figure 4. Determination of the Correlation Coefficient $1/B_L$ for Levy's Equation

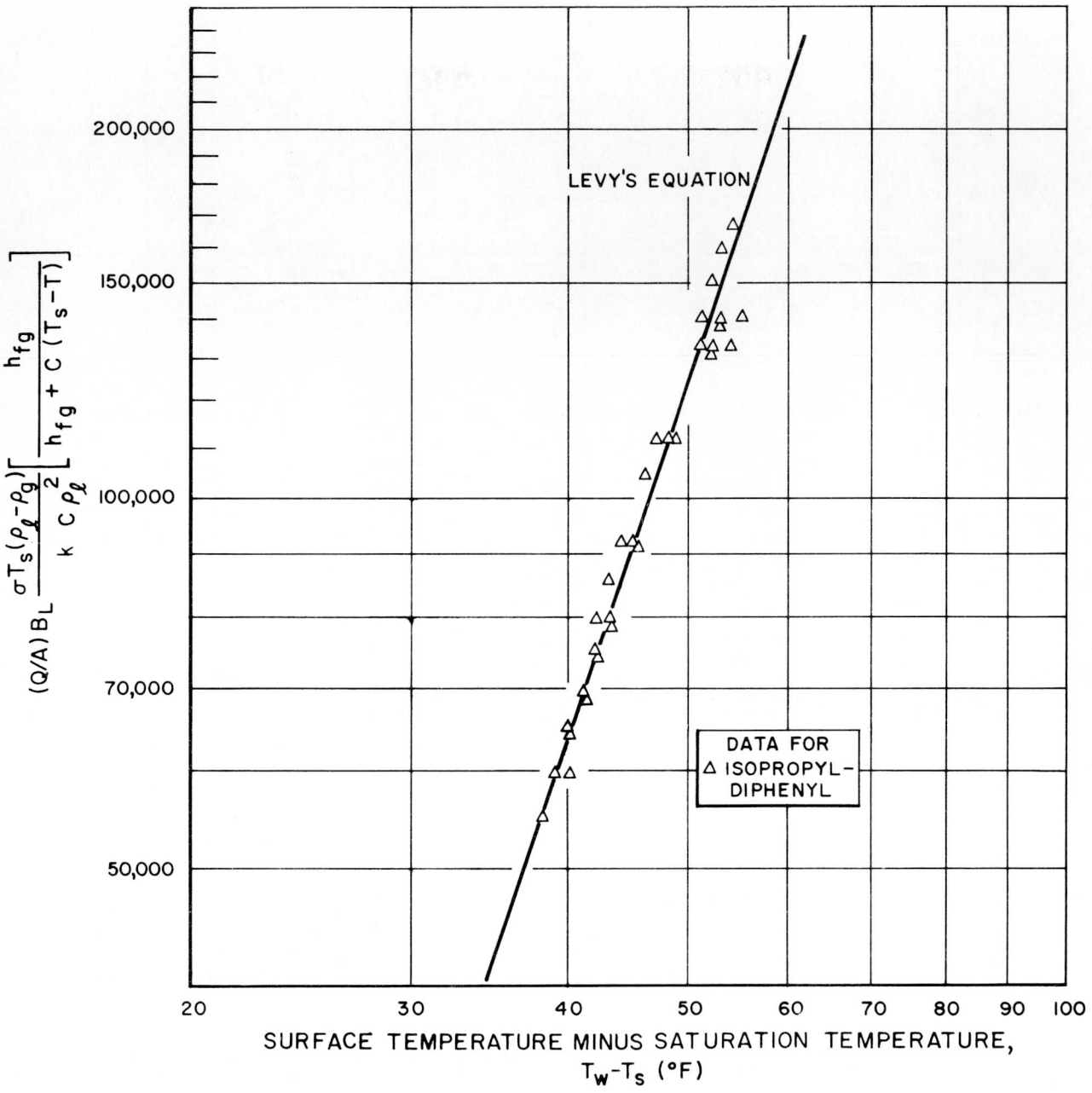

Figure 5. Correlation of Boiling Heat Transfer Data for Isopropyl Diphenyl with Levy's Equation

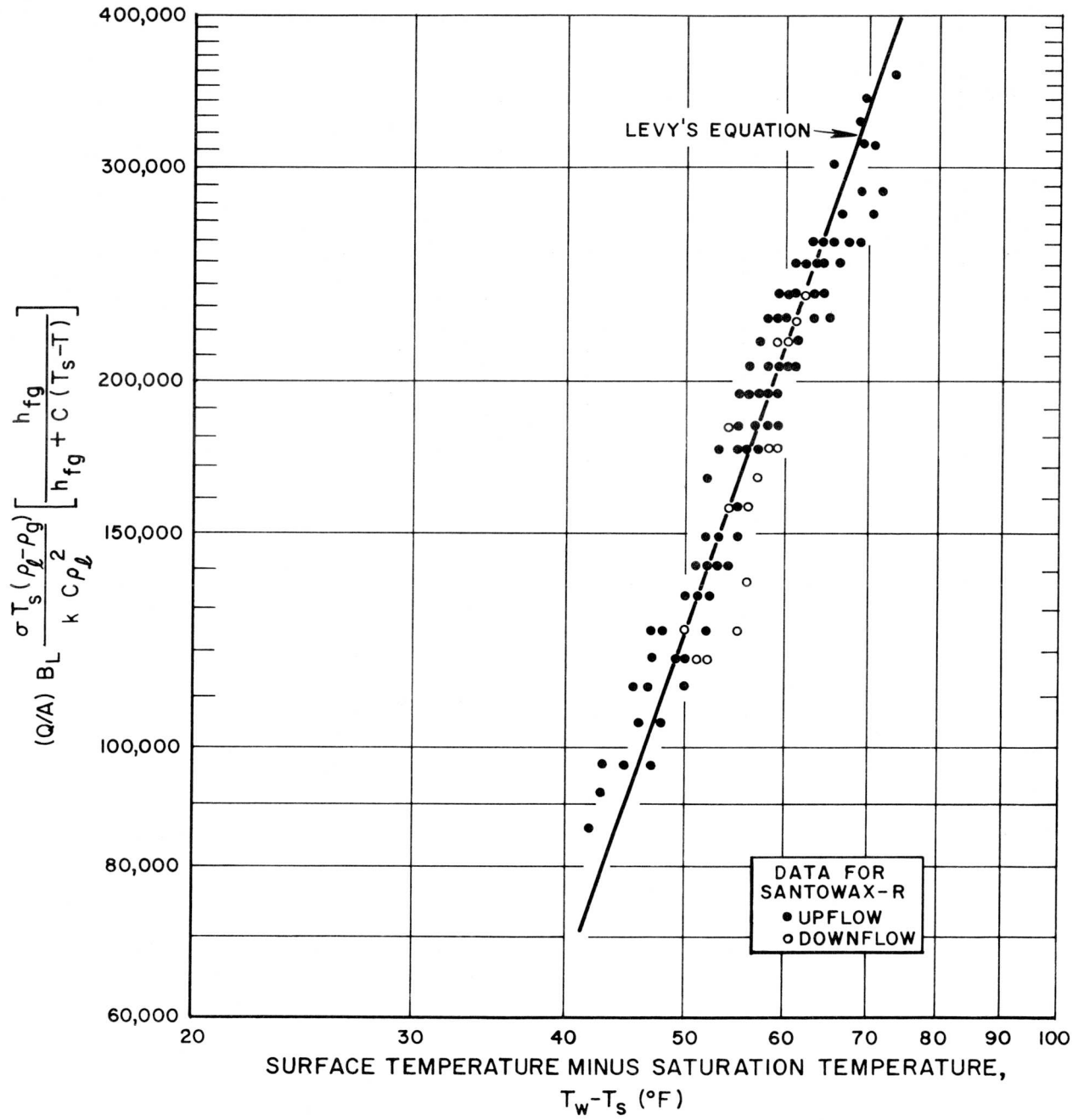

Figure 6. Correlation of Boiling Heat Transfer Data for Santowax-R with Levy's Equation

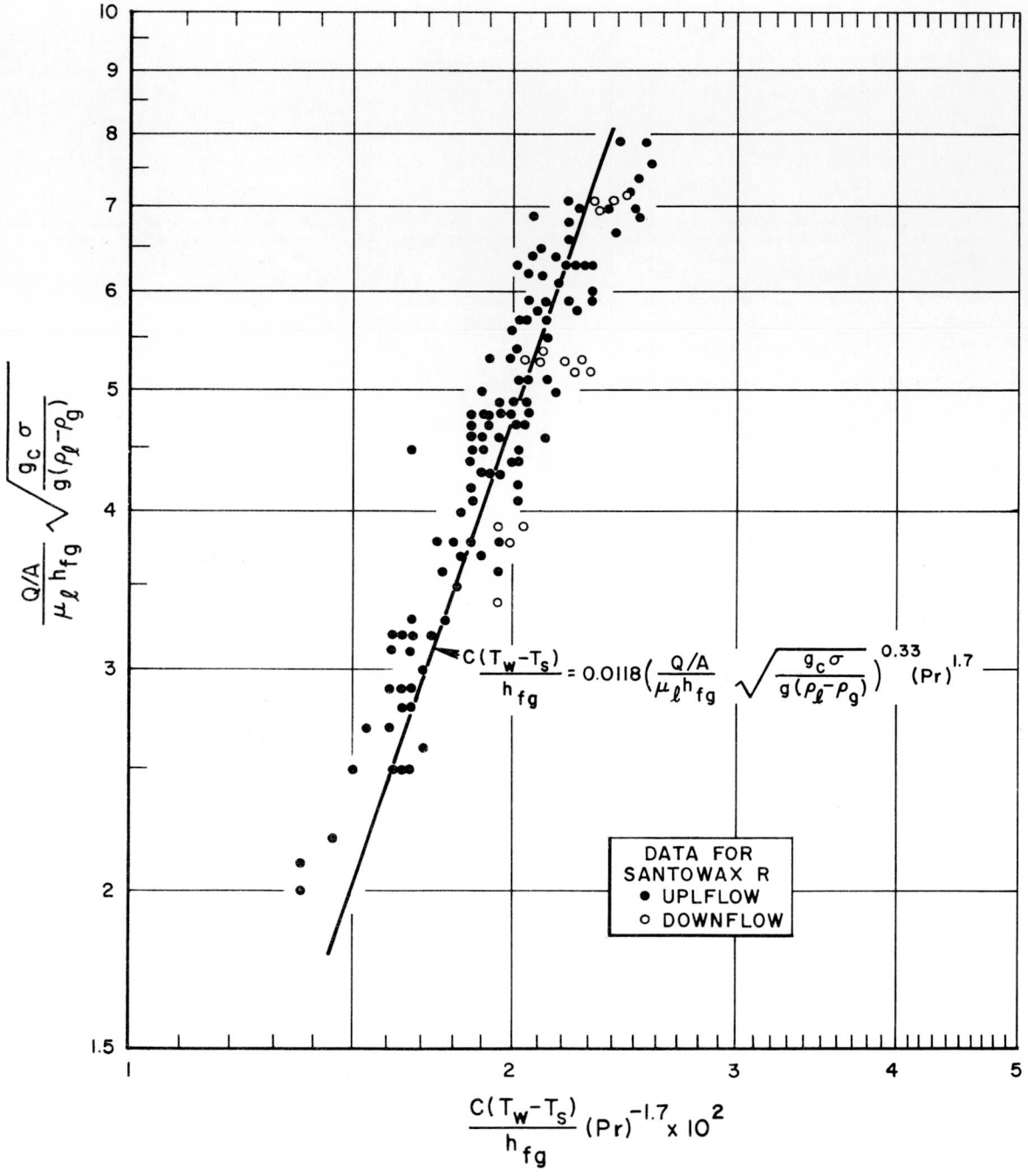

Figure 7. Correlation of Boiling Heat Transfer Data for Santowax-R with Rohsenow's Equation

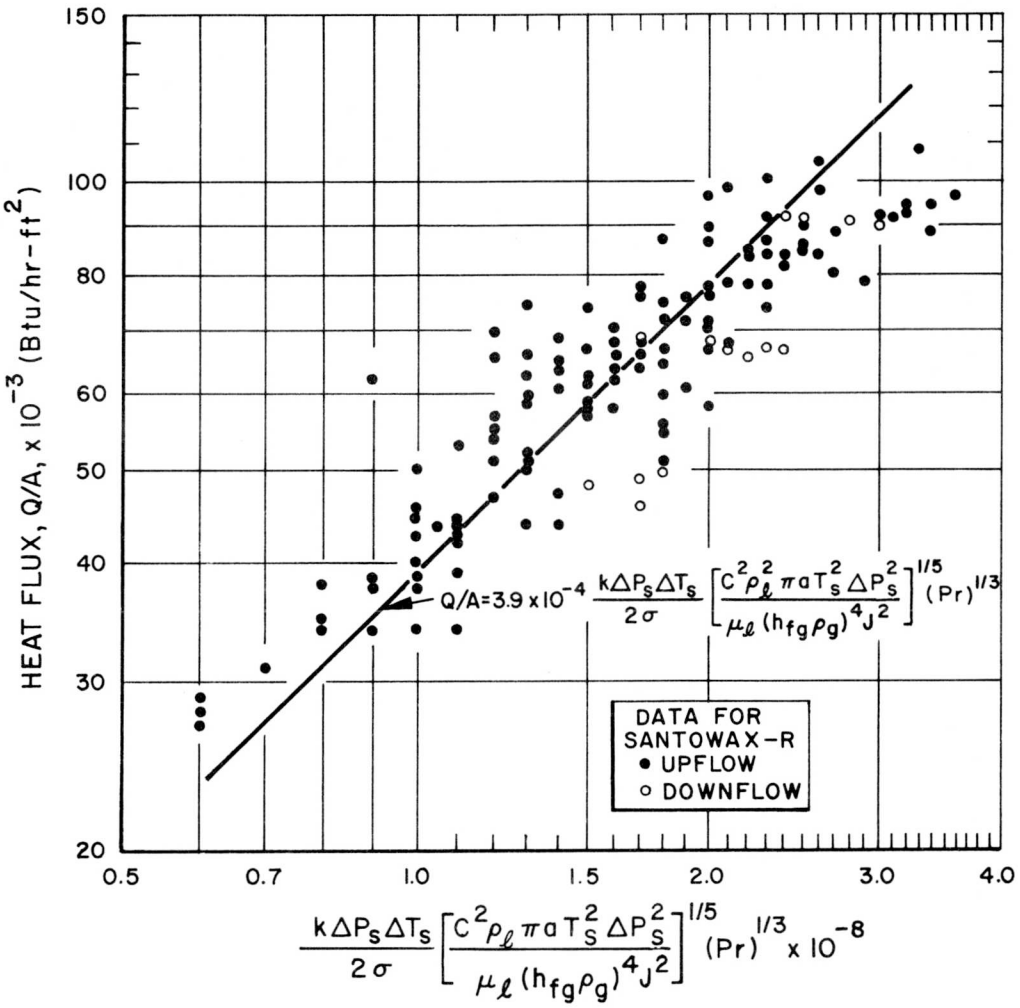

Figure 8. Correlation of Boiling Heat Transfer Data for Santowax-R with Forster-Greif Correlation-I

B. VOID FRACTION

The range of subcooling for which the void fraction of Santowax-R was determined was 0 to 50°F. The range of vapor quality was 0 to 0.17. The void fraction results corresponding to a $\Delta T_{sub} > 8°F$ and to the pressure range of 15 to 28 psia were correlated by the following equation:

$$\alpha = 1.55 \left[\frac{Q/A - h(T_w - T)}{h^2 (T_s - T)} \right] \left[\frac{Prk}{s/4} \right] \qquad \ldots (1)$$

This equation has the general form of the Maurer's equation,[9] based on work by Griffith, Clark, and Rohsenow.[10] The arbitrary constant of 1.55 was determined from a best fit of the data. Correlation of the experimental results for both upflow and downflow with the above equation is shown in Figure 9. The results are presented in Table A-3. Over the relatively narrow range of pressures investigated, no significant pressure effect was observed on the void fraction values corresponding to subcooled boiling. For conditions of bulk temperature at or near saturation, the void fraction results were correlated by the following equation:

$$\frac{\alpha}{1 - \alpha} = K \frac{\left[Q/A - h(T_w - T) \right] S \rho_\ell}{G A_F h_{fg} \rho_g} \qquad \ldots (2)$$

The average value of K is 0.22 obtained by a best fit of the data. It represents the grouping $\frac{K_o \Delta L v_\ell}{v_g}$, with the units of length. Correlation of the experimental results for both upflow and downflow with this equation is shown in Figure 10. The results are presented in Table A-4.

The void fraction results corresponding to equilbrium bulk boiling up to a quality of 0.17 were correlated with the modified Martinelli parameter:[11]

$$X = \left(\frac{1 - x}{x} \right)^{0.875} \left(\frac{\mu_\ell}{\mu_g} \right)^{0.125} \left(\frac{\rho_g}{\rho_\ell} \right)^{0.5} . \qquad \ldots (3)$$

Comparison of the experimental results for both upflow and downflow with the Lockhart-Martinelli curve[12] is given in Figure 11. The results of this survey are listed in Table A-5.

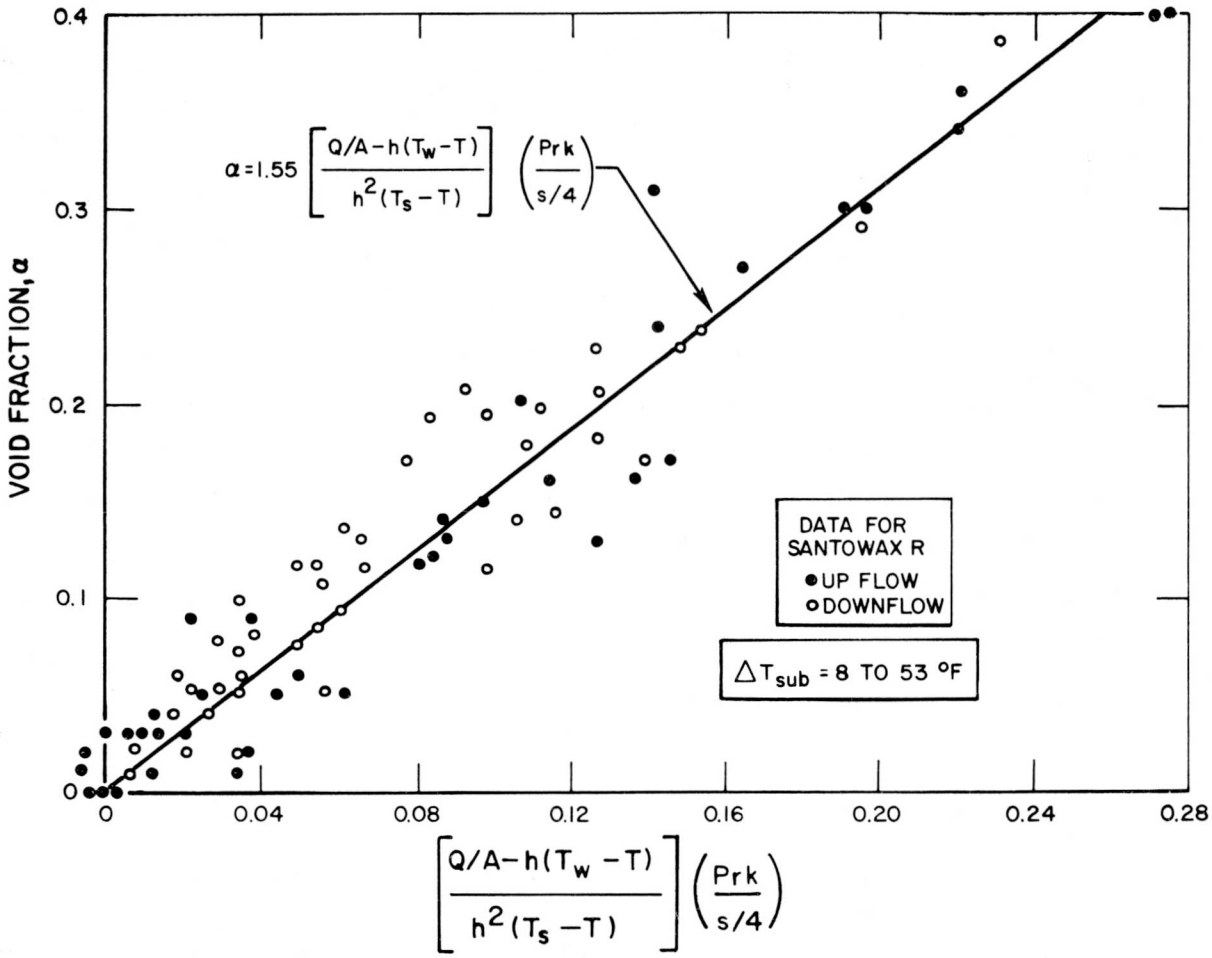

Figure 9. Correlation of Subcooled Boiling Void Fraction for Santowax-R

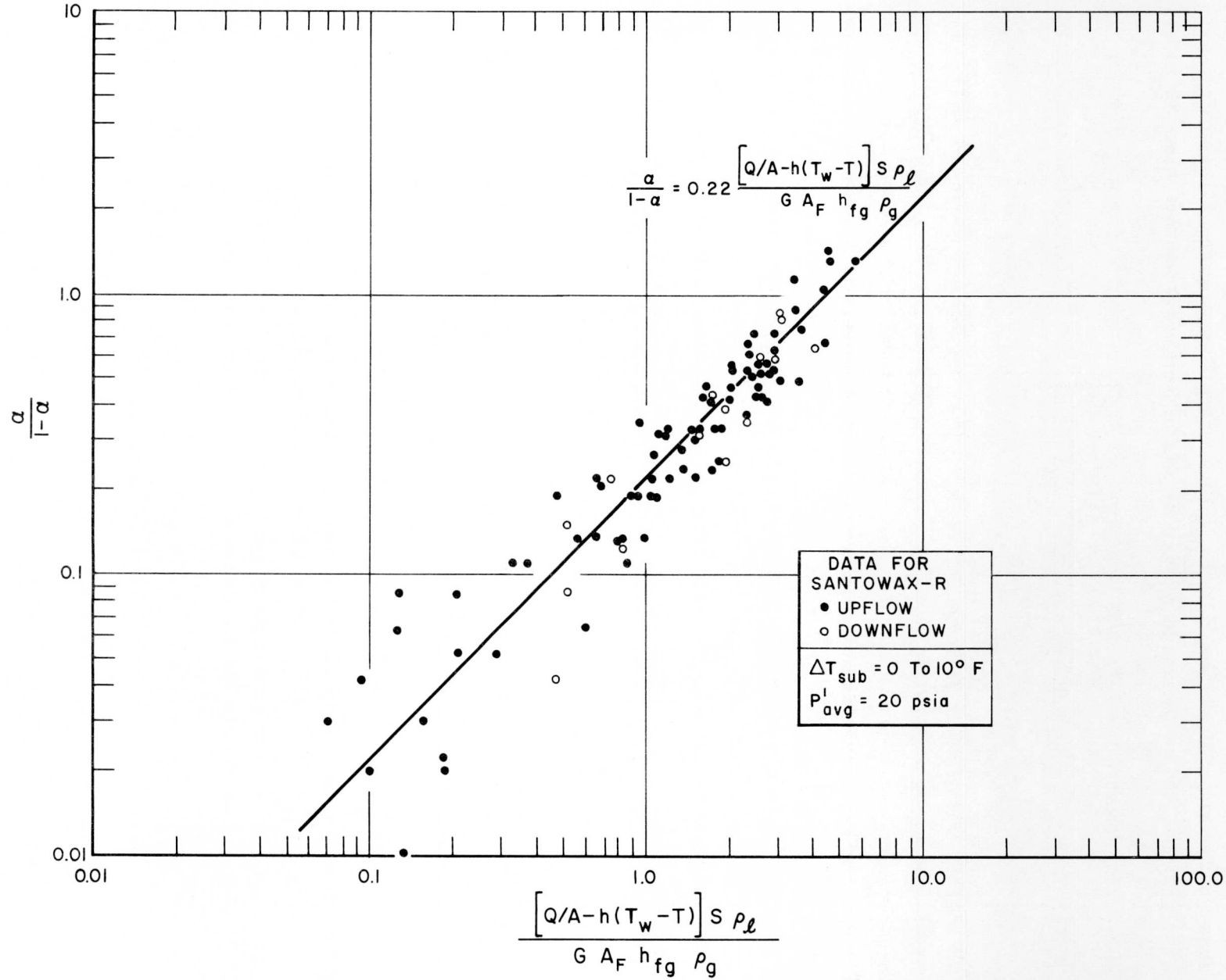

Figure 10. Correlation of Santowax-R Void Fraction at or Near Saturated Boiling

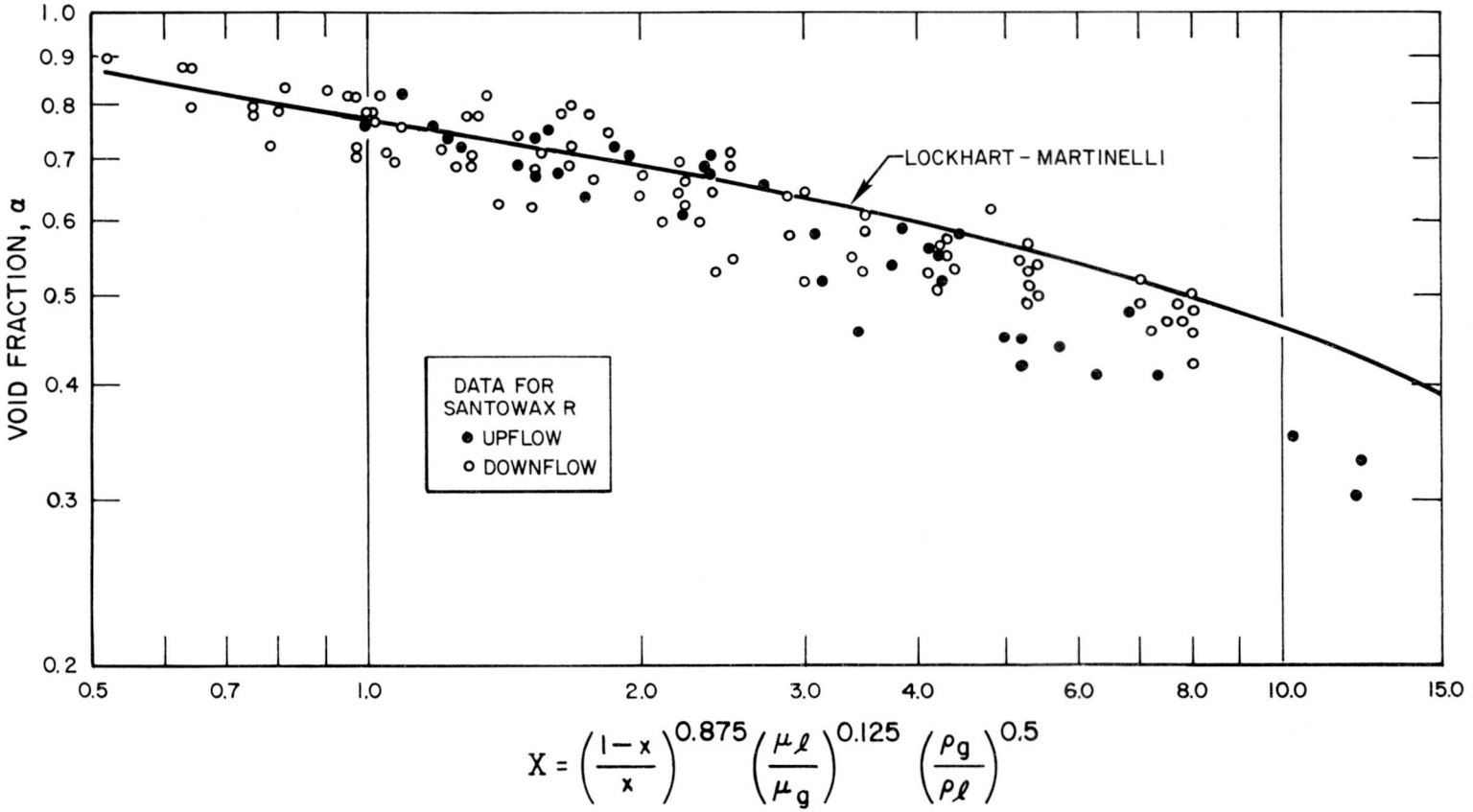

Figure 11. Correlation of Void Fraction Data for Santowax-R with the Martinelli Parameter X

IV. DISCUSSION OF RESULTS

The mechanisms of heat transfer and void formation during nucleate boiling are dependent on the interrelation of several independent variables. In addition, surface conditions, surface material, and channel geometry have been found to affect these mechanisms to a certain degree in various instances.[7,13,14,15]

Attempts at assessing the relative effect of the several variables, with the object of developing generalized theoretical models, have not been completely successful to date. This is particularly the case for the mechanism of void formation in the subcooled and low-quality boiling regions.

A. BOILING HEAT TRANSFER

For the mechanism of nucleate boiling heat transfer, various models and correlations have been proposed. Generally, these correlations require experimental constants for direct application to a particular fluid and/or system.

Three boiling heat transfer equations taken from the literature were used to correlate the data: (1) Levy's[6] equation which uses a correlation constant dependent on pressure and requires evaluation at several pressures in order to achieve the proper pressure dependence; (2) Rohsenow's[7] equation which has a correlation constant evaluated at one pressure, the pressure dependence of boiling heat transfer is "built" into this equation by way of the grouping of physical properties which vary with pressure; and (3) Forster-Greif's[8] correlation-I. Both Levy's equation and Rohsenow's equation have a heat flux depending on wall superheat to the third power; however, the physical properties of the coolant are taken into account differently. The scatter of the correlated data (Figures 6, 7, and 8) shows that Levy's equation correlates the data better than Rohsenow"s equation which in turn correlates the data better than Forster-and-Greif's equation. Levy's method allows for greater variation of boiling heat transfer with pressure.

The value of 0.0118 obtained for C_{sf} in Rohsenow's equation compares well with some of the values listed in Reference 7. For Example:

Fluid-Heating Surface	C_{sf}
Water-platinum	0.013
Benzene-chromium	0.010
N-pentane-chromium	0.015

Any of these values could have been used to obtain reasonable predictions of wall superheat using Santowax-R as a coolant.

B. VOID FRACTION

Local void fraction in a channel, for steady state conditions of forced circulation nucleate boiling and uniform heat flux, increases along the channel length as the coolant enthalpy increases. Observation of the void fraction profiles for boiling water channels where the flowing coolant initially subcooled undergoes vaporization to appreciable values of quality has indicated the existance of three regions of vapor formations. These regions have been used as the basis for the predictions of void fractions in coolant channels of boiling water reactors.[9] Essentially the same regions have been observed in the analysis of the present investigation on Santowax-R void fractions. However, the actual ranges of the observed regions were found to differ widely for the two systems. This is probably due to the significant differences in the values of such physical properties as the heat of vaporization, the thermal conductivity, and the vapor density of the two fluids at their respective operating conditions of pressure and temperature.

Based on the present results and limited by the operating ranges investigated, the void fraction regions for Santowax-R have been classified as follows: Region I covers subcooled boiling for coolant subcooled greater than 8°F, approximately; Region II covers the transition from subcooled to equilibrium bulk boiling; and Region III covers equilibrium bulk boiling at qualities greater than 0.005, approximately.

1. Subcooled Boiling Void Fraction

The results of the subcooled boiling void fraction experiments indicate the time-averaged volume-fraction of Santowax-R vapor at a specific point in the channel to be a function of heat flux, mass velocity, and degree of subcooling. Other conditions being constant, the volume of voids in the channel increases with increase in heat flux, increases with lower subcooling, and decreases with increasing mass velocity. This is in qualitative agreement with the observed behavior of void formation for the subcooled boiling heat transfer to water with forced convection reported by Gunther[16] and other investigators.[9,15,17] Satisfactory correlation of the data (see Figure 9) was obtained by use of Maurer's

equation.[9] This equation is based on the semitheoretical model of Griffith, Clark, and Rohsenow,[10] with a correlation constant determined from the data. Considering that the validity of this model is at best questionable in describing the Santowax-R vapor formation at the subcooled boiling conditions investigated, the satisfactory correlation of the data with this equation was not expected. Among the most obvious discrepancies of this correlation as applied to this situation are: the void volume corresponding to the growing cycle of the bubble is not accounted for, the range of void thickness measured far exceeds the maximum "one-bubble diameter" limit of the model, and a relatively low subcooling range is involved. In light of these discrepancies, the successful correlation of the data could be interpreted as the result of the main variables affecting void fraction being indirectly accounted for in the proper relationship, rather than as the overall correlation being the true analytical representation of the mechanisms involved. Careful evaluation of this possibility has led to the development of a more general model which has the general form of Maurer's equation without its main limitations.

Consider the case where the total heat flux of a forced circulation subcooled boiling system is of the same order of magnitude as the heat flux corresponding to the onset of nucleate boiling. In this case (see Reference 10), the total heat flux is given by:

$$Q/A = (Q/A)_{nb} + (Q/A)_b \quad , \qquad \ldots (4)$$

and the boiling heat flux by:

$$(Q/A)_b = Q/A - h(T_s - T) \quad ; \qquad \ldots (5)$$

or, as modified by Maurer (see Reference 9),

$$(Q/A)_b = Q/A - h(T_w - T) \quad . \qquad \ldots (6)$$

For the case where the condensing heat flux of the system is approximately equal to the boiling heat flux, $(Q/A)_b \cong (Q/A)_c$, the following relationship applies:

$$(Q/A)_c = Q/A - h(T_w - T) = h_c \frac{A_c}{A}(T_s - T) \quad , \qquad \ldots (7)$$

where h_c is the average condensing heat transfer coefficient of the bubbles and A_c is the average equivalent heat transfer area of the condensing bubbles. Generally, the average volume of the condensing bubbles may be related to the average surface area of the bubbles by an approximation of this type:

$$V_c = B_o A_c R_m \quad , \qquad \ldots (8)$$

where, B_o is a dimensionless geometrical factor, and R_m is the maximum average bubble radius. Combining Equation 8 and 7, we obtain,

$$Q/A - h(T_w - T) = h_c \frac{V_c}{B_o R_m A}(T_s - T) \quad . \qquad \ldots (9)$$

For the case where the average volume corresponding to the growing, noncondensing bubbles, V_{gr}, is negligible in comparison with V_c; or, for the case where V_{gr} and V_c are directly proportional to each other, Equation 9 can be used to correlate total void volume, V_t,:

$$\frac{V_t}{A} = \frac{B'_o R_m \left[Q/A - h(T_w - T)\right]}{h_c (T_s - T)} \qquad \ldots (10)$$

or to correlate void fraction, α, in a circular geometry:

$$\alpha = \frac{V_t/A}{s/4} = \frac{B''_o R_m \left[Q/A - h(T_w - T)\right]}{s\, h_c (T_s - T)} \qquad \ldots (11)$$

where s is the channel diameter and B''_o is a dimensionless proportionality constant. The usefulness of Equation 11 is limited by the lack of correlations to predict the value of average condensing heat transfer coefficient, h_c, and the value of maximum average bubble radius, R_m. A general approximation however,

may be attempted which can be used as a guide for the correlation of void fraction data; that is, for relatively small ranges of operating temperature and pressure, R_m is a function of velocity and subcooling[16] as follows:

$$R_m \sim \frac{1}{(G)^a (T_s - T)^b} \quad . \qquad \ldots (12)$$

For small ranges of temperature, it is anticipated that h_c is essentially a function of mass velocity only, $h_c \sim (G)^c$. Based on the above relationships an approximate alternate of Equation 11 for correlation of subcooled boiling void fraction data, in terms of the variables affecting it, can be obtained:

$$\alpha = \frac{B\left[Q/A - h(T_w - T)\right]}{s(G)^m (T_s - T)^n} \quad , \qquad \ldots (13)$$

where B is an empirical correlation coefficient for the particular system, and m and n are empirically determined exponents.

For the case of m = 1.6 and n = 1 approximately, this equation is equivalent to Maurer's equation. Although the present data substantiate the validity of the correlation presented with the above values of m and n, this parameter survey is limited and further experimental verification and/or improvement of the modified model is warranted.

2. Void Fraction at or Near Saturation Temperature

For conditions of bulk temperature at or near saturation, the void fraction of Santowax-R in the channel tested has been observed to be essentially a function of heat flux and mass velocity. Over the narrow range of pressure investigated, no significant effect of pressure on the void fraction is apparent. Attempts to correlate the data in terms of total heat flux proved to be unsuccessful. As in the case of Region I, the void fraction data have been correlated in terms of the net boiling heat flux.[10]

For conditions of bulk temperature at or near saturation and a constant pressure, the void fraction of Santowax-R flowing in the uniformly heated channel has been observed to be a function of heat flux and mass velocity. Over this range of low subcooling, the void fraction does not appear to be affected significantly by the Δt_{sub} driving force; at least not to the extent observed in the higher subcooling range of Region I. These observations lead to speculations on the possibility of a mechanism other than the condensing mechanism being the controlling factor for the void fraction in this region.

The relationship between void fraction and the weight fraction of vapor at a point along the channel based on the mass of fluid present is:

$$\frac{\alpha}{1 - \alpha} = \frac{x^+}{1 - x^+} \cdot \frac{\rho_\ell}{\rho_g} \quad . \qquad \ldots(14)$$

This is an absolute relationship which applies to both equilibrium and nonequilibrium liquid-vapor systems. Values of x^+ calculated with Equation 14 for the tabulated void fraction data at or approaching saturation are found not to exceed 0.015. Consequently, Equation 14 may be approximated for the case considered by:

$$\frac{\alpha}{1 - \alpha} = x^+ \frac{\rho_\ell}{\rho_g} \quad . \qquad \ldots(15)$$

For nonequilibrium conditions, the value of x^+ at a given point along the heated channel is not an accumulated value depending on total heat addition as in the case of equilibrium bulk boiling. It is rather, a local value depending on the interrelation of the mechanisms of bubble formation and condensation. Consider, however, a low subcooling system having a temperature field whereas the bubbles formed exist in a noncondensing medium for a time considerably longer than the condensing time. In this case, it could be postulated that the time-average weight fraction of vapor is essentially dependent on the relative ability of the system to vaporize a fraction of the flowing fluid. This is somewhat analogous to the situation of equilibrium bulk boiling where x^+ is expressed by:

$$\frac{x^+}{1 - x^+} = \frac{x}{1 - x} \cdot \frac{v_\ell}{v_g} \quad ; \qquad \ldots(16)$$

with x determined from a heat balance on the total bulk boiling channel length, ΔL_b,

$$x = \frac{Q/L\ \Delta L_b}{Wh_{fg}} \quad . \qquad \ldots(17)$$

By application of this method to the nonequilibrium situation considered, and by assuming that the vapor generation rate at moderate heat fluxes is proportional to the boiling heat flux, $(Q/A)_b$, as defined in the preceding section, the following relationship is obtained:

$$x = \frac{K_o(Q/A)_b S\Delta L}{GA_F h_{fg}} \quad , \qquad \ldots(18)$$

Where ΔL corresponds to an arbitrary increment of length rather that total boiling channel length and x is the noncumulative time average weight fraction of vapor (a function only of the percent of flowing fluid vaporized at a given point). For a small value of x^+ and x, Equation 16 may be approximated as follows:

$$x^+ = x\frac{v_\ell}{v_g} \quad . \qquad \ldots(19)$$

By combining Equations 15, 18, 19, and the relationship for $(Q/A)_b$:

$$\frac{\alpha}{1-\alpha} = \frac{K_o\left[Q/A - h(T_w - T)\right] S\Delta L}{GA_F h_{fg}} \cdot \frac{v_\ell}{v_g} \cdot \frac{\rho_\ell}{\rho_g} \quad . \qquad \ldots(20)$$

If a relatively constant value of v_ℓ/v_g be assumed for the situation considered, Equation 7 will reduce to Equation 2:

$$\frac{\alpha}{1-\alpha} = \frac{K\left[Q/A - h(T_w - T)\right] S\rho_\ell}{GA_F h_{fg}\rho_g} \quad ,$$

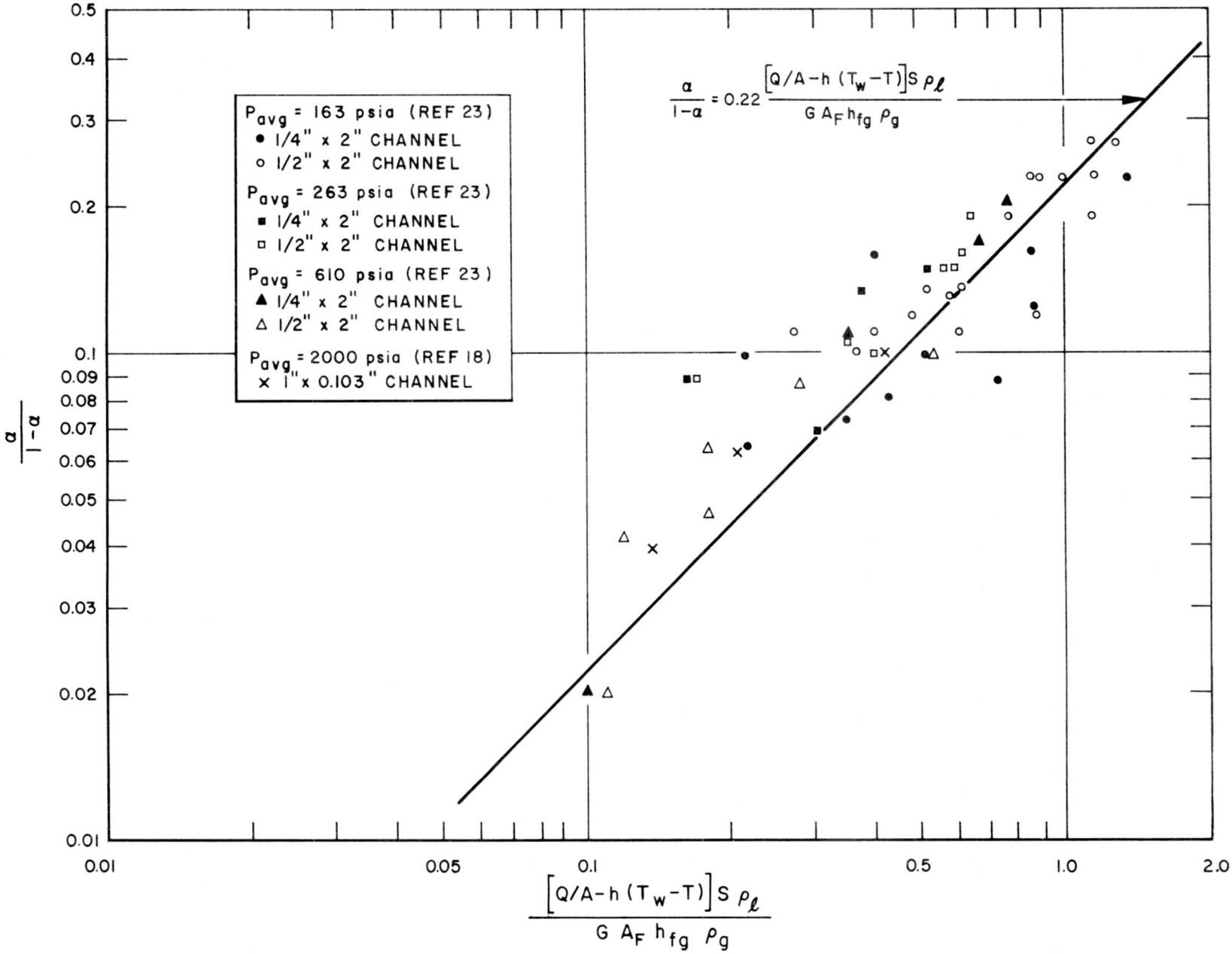

Figure 12. Correlation of Water Vapor Void Fraction at or Near Saturated Boiling

where the correlation coefficient K represents the grouping $K_o(\Delta L v_\ell / v_g)$ with the units of length.

Correlation of the void fraction data of Santowax-R with Equation 2, illustrated in Figure 10, tends to substantiate the validity of the above derivation and assumptions. The average value of K corresponding to the data presented is 0.22 ft. The value of the correlation constant represents the approximate average of the data points, correlated in Figure 10. The scatter of the data from the average is within the overall experimental accuracy. The data represent subcoolings in the range of 0 to 10°F with most of the data points closer to 0°F subcooling. The value of subcooling for the transition from Region I to Region II is not a constant value. For the conditions investigated, it varies in the approximate range 6 to 10°F, and the applicable region is selected as the one which predicts the lower value of void fraction.

For a limited range of equilibrium quality (up to x = 0.005), the void fraction continues to be a function of heat flux and mass velocity. Void fraction values in this narrow range can be predicted by a straight line extrapolation from the void fraction value corresponding to 0°F subcooling to the void fraction value corresponding to x = 0.005, as predicted by the Martinelli method discussed under Region III. This is necessary due to the fact that the Martinelli model predicts zero void fraction at x = 0.

The dimensionless and generalized character of the correlation developed for this region suggests the possibility of application to other systems and geometries. As an independent check on the validity and possible application of Equation 2 to other systems and geometries, void fraction data for boiling water at or near saturation temperatures have been correlated by this method. Data for water at moderate heat fluxes, for which the relationship of $(Q/A)_b$ applies have been obtained in References 23 and 18. The data correspond to three different geometries, four pressure ranges, and wide ranges of flow rates and heat fluxes. The values of h were calculated by the Dittus-Boelter equation,[13] and the wall temperature, T_w, was determined by the Jens-Lottes correlation.[15] Considering the wide ranges of operating variables, the possibility of errors introduced in calculating the value of $(Q/A)_b$, and possible experimental inaccuracies, the correlation of the data (see Figures 12 and 13) is surprisingly satisfactory.

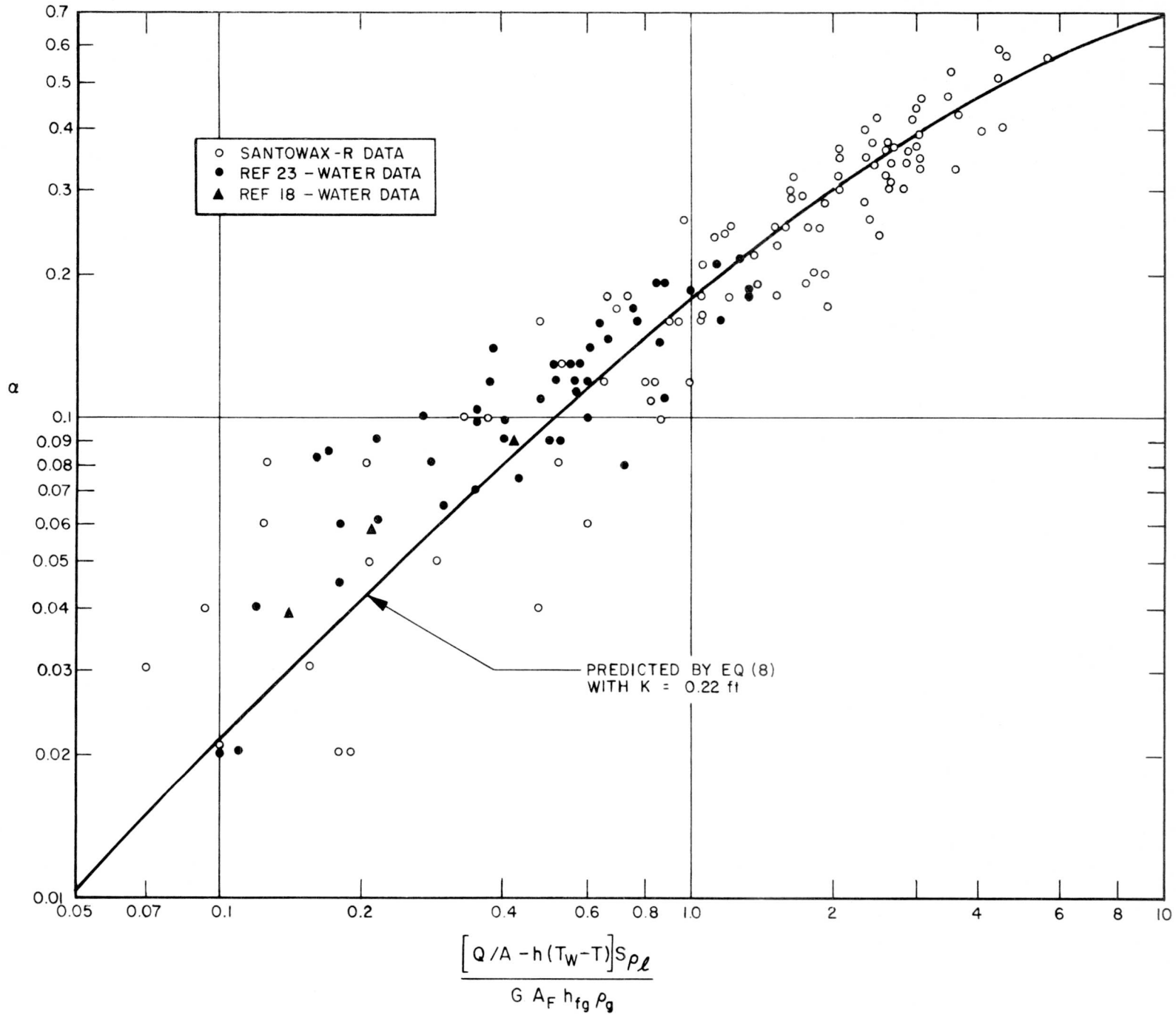

Figure 13. Comparison of Void Fraction Data With Predicted Values From Equation 2

As an additional check, boiling water data at high heat fluxes[9, 18] were correlated with Equation 2. For this case, $(Q/A)_b$ is approximately equal to Q/A and Equation 2 can be simplified to:

$$\frac{\alpha}{1 - \alpha} = \frac{K(Q/A)S\rho_\ell}{GA_F h_{fg} \rho_g} \quad .$$

These data, presented in Figure 14, show a pressure effect on the value of K that was not apparent from the data at the moderate heat fluxes ($Q/A < 100{,}000$ Btu/hr-ft^2). At a given pressure, satisfactory correlation of the data is obtained with Equation 2. This tends to further substantiate the validity of the basic model; however, further investigation and analysis are still required before definite conclusions may be made on its generality or limitations.

3. Void Fraction for Equilibrium Bulk Boiling

This region covers the void fraction results of Santowax-R for equilibrium bulk boiling at qualities greater than 0.005, approximately. In this region, the void fraction becomes essentially independent of heat flux and mass flow rate, and can be correlated with the Martinelli model of varying slip ratio. The data have been correlated in terms of the Martinelli parameter X[11] and compared with the Lockhart-Martinelli curve in Figure 11.

The agreement of the data is good at the lower value of X (higher qualities). At the higher X values (lower qualities), the data is somewhat lower than the predicted values. This apparent discrepancy can be caused by several factors. First, the Lockhart-Martinelli curve is based on data obtained for isothermal, two-phase, two-component flow in horizontal pipes. The difference of flow direction alone can possibly account for the lower vertical flow void fraction results. This trend has been previously observed[19] in the data of Dengler[20] and of Egan[18] investigating steam-water flow in vertical pipes. Another factor can be the uncertainty related to the determination of quality-value of Santowax-R corresponding to a given measurement of void fraction.

Santowax-R is a mixture of several components. As boiling occurs, the concentration of more volatile components will gradually decrease in the liquid phase with consequent increase of the saturation temperature. The equilibrium

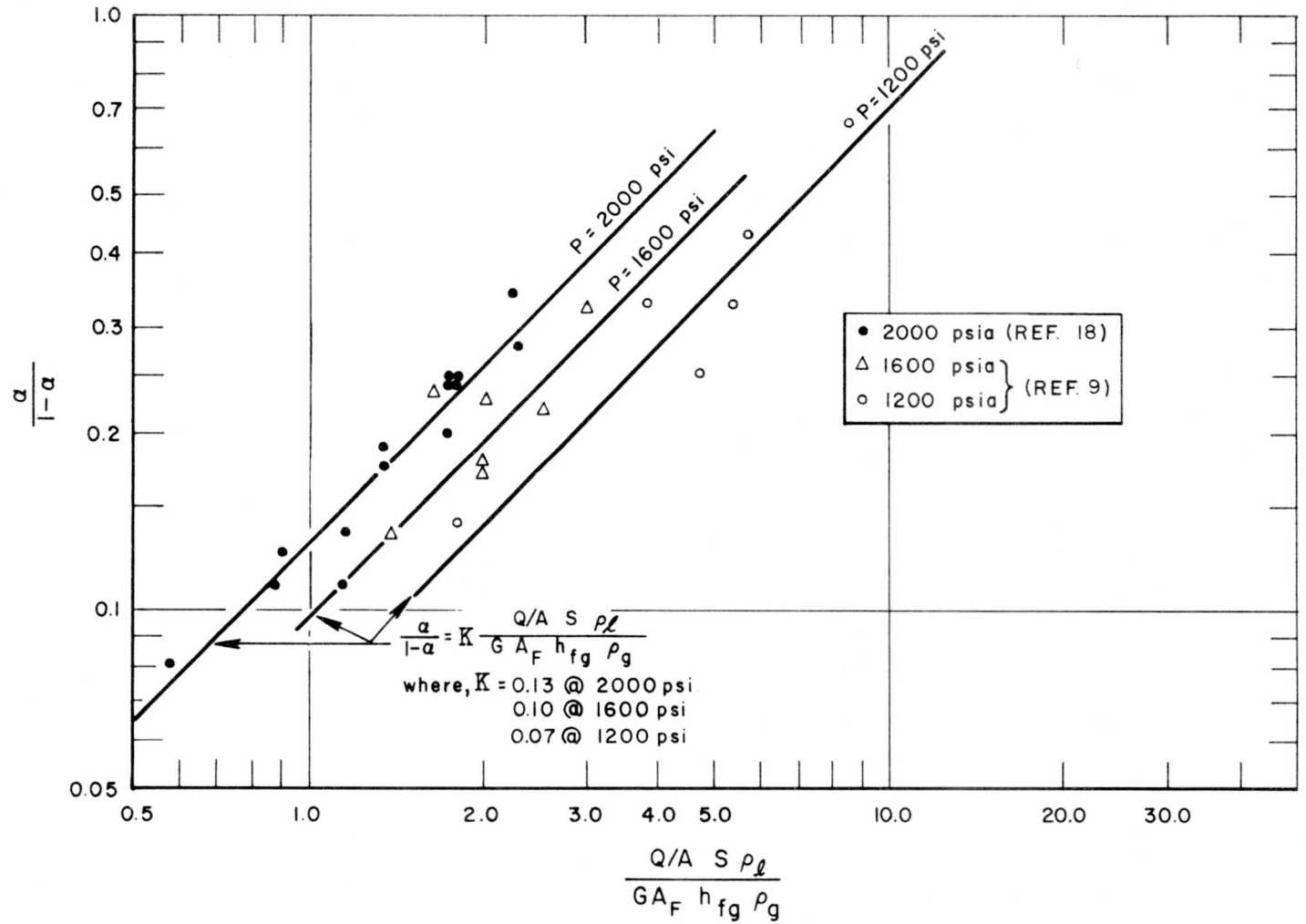

Figure 14. Correlation of Water Vapor Void Fraction at or Near Saturated Boiling - High Heat Fluxes

phase diagram of this multicomponent system is not presently known; hence, qualities were determined on the basis of the initial saturation temperature. This would give higher-than-actual values of quality, causing a shift of the data from the Lockhart-Martinelli curve. Another uncertainty in the determination of the quality-value of Santowax-R is related to the experimental accuracy. This uncertainty is estimated to be equivalent to a value of 0.005 quality, on the basis of possible errors in temperature and absolute pressure measurements.

The void fraction results have been evaluated also in terms of slip ratio, v_g/v_ℓ, determined as follows:

$$SR = v_g/v_\ell = \left(\frac{x}{1 - x}\right)\left(\frac{1 - \alpha}{\alpha}\right)\left(\frac{\rho_\ell}{\rho_g}\right) \quad .$$

The effect of quality on the slip ratio at the pressure ranges investigated is summarized in Figure 15. The results are in qualitative agreement with the results of boiling water experimentation.[15]

During the bulk boiling survey, only a narrow range of mass flow rates has been investigated because of operating limitations. Over the range tested, no effect of flow rate on the slip ratio of Santowax-R was observed. However, this is not considered conclusive because of the limited range investigated.

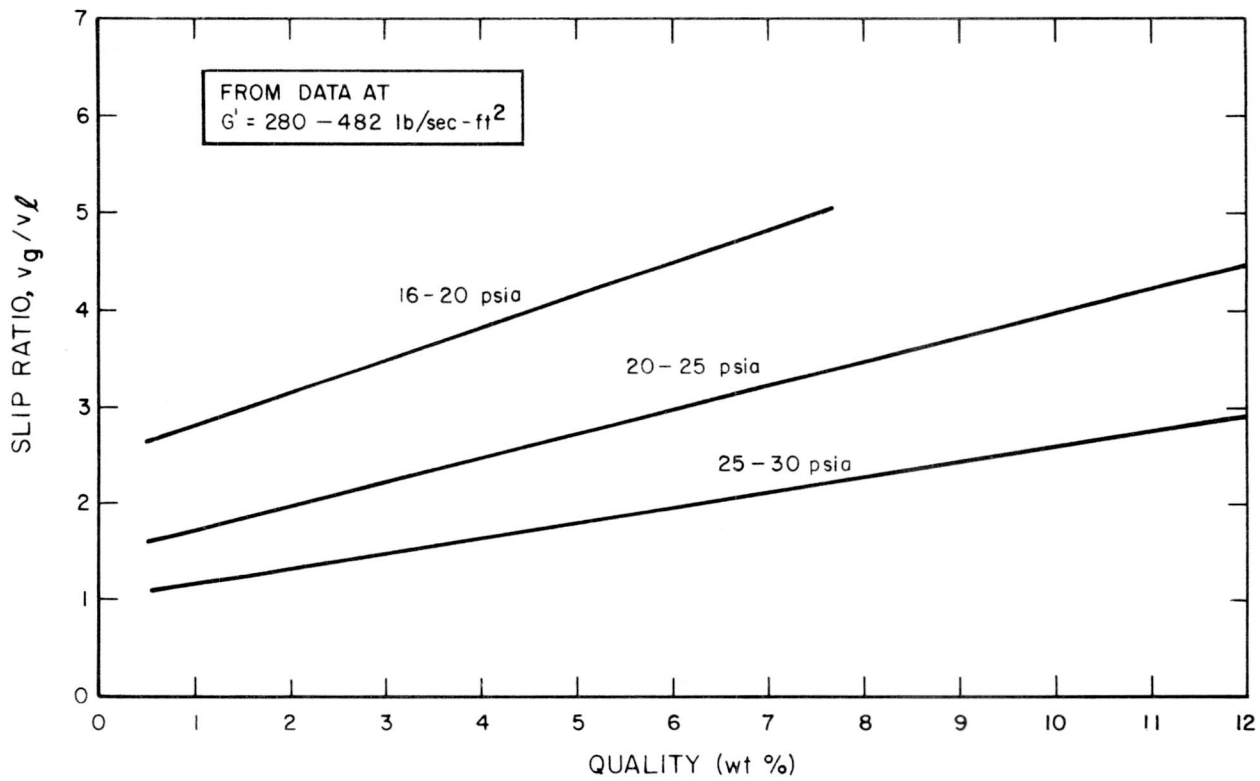

Figure 15. Slip Ratio of Santowax-R as a Function of Quality at Various Pressure Ranges

V. REFERENCES

1. W. P. Kunkel, "A Survey of the Assumptions and Areas of Uncertainty in OMR Hazards Evaluation," NAA-SR-TDR-6006, 1961.

2. R. C. Noyes, F. Bergonzoli, and J. E. Gingrich, "FUGUE," NAA-SR-5958, 1961.

3. F. J. Halfen and F. Bergonzoli, Boiling Depressurization Transients," NAA-SR-9033, 1964.

4. F. Bergonzoli, W. H. Wickes, E. E. Stoner, and F. J. Halfen, "Flow Stability Test Loop," NAA-SR-8610, 1963.

5. J. H. Kendron, E. E. Stoner, and G. M. Taylor, "Dynamic Void Fraction Measurement System," NAA-SR-7875, 1963.

6. S. Levy, "Generalized Correlation of Boiling Heat Transfer," ASME Paper No. 58-HT-8, 1958.

7. W. M. Rohsenow, "A Method of Correlating Heat-Transfer Data for Surface Boiling of Liquids," Trans. ASME, Vol 74, 969, 1952.

8. H. K. Forster and R. Greif, "Heat Transfer to a Boiling Liquid - Mechanism and Correlations," ASME Paper No. 58-HT-11, 1958.

9. G. W. Maurer, "A Method of Predicting Steady-State Boiling Vapor Fractions in Reactor Coolant Channels," WAPD-BT-19, 1960.

10. P. Griffith, J. A. Clark, and W. M. Rohsenow, "Void Volumes in Subcooled Boiling Systems," ASME Paper No. 58-HT-19, 1958.

11. R. C. Martinelli and D. B. Nelson, "Prediction of Pressure Drop During Forced Circulation Boiling of Water," Trans. ASME, Vol 70, 695, 1948.

12. R. W. Lockhart and R. C. Martinelli, "Proposed Correlation of Data for Isothermal Two-Phase, Two-Component Flow in Pipes," Chem. Engr. Progress, Vol 45, 39, 1949.

13. W. H. McAdams, "Heat Transmission," 3rd Edition, 1954.

14. H. Buchberg, et al., "Studies in Boiling Heat Transfer - Final Report," COO-24, 1951.

15. P. A. Lottes, et al., "Boiling Water Reactor Technology Status of the Art Report - Volume I. Heat Transfer and Hydraulics," ANL-6561, 1962.

16. F. C. Gunther, "Photographic Study of Surface Boiling Heat Transfer to Water With Forced Convection," Trans. ASME, Vol 73, 115, 1951.

17. C. P. Costello, "Aspects of Local Boiling Effects on Density and Pressure Drop," ASME Paper No. 59-HT-18, 1959.

18. R. A. Egen, D. A. Dingee, and J. W. Chastain, "Vapor Formation and Behavior in Boiling Heat Transfer," BMI-1163, 1957.

19. W. A. Wahl, "Compilation of Two Phase Flow Data," NAA-SR-TDR-4339, 1959.

20. C. E. Dengler, Sc. D. Thesis in Chemical Engineering, Massachusetts Institute of Technology, 1952.

21. Monsanto Booklet, Physical Properties of Monsanto Radiation Resistant Fluids.

22. R. H. J. Gercke, F. C. Silvey, and G. Asanovich, "The Properties of Santowax-R (Mixed Terphenyl Isomers) As Organic Moderator-Coolant," NAA-SR-MEMO-3223, 1959.

23. J. F. Marchettere, et al., "Natural and Forced-Circulation Boiling Studies," ANL-5735, 1960.

VI. NOMENCLATURE

a = Thermal diffusivity of liquid, ft^2/hr

A = Heat transfer area, ft^2

A_F = Flow area, ft^2

B_L = Correlation coefficient in Levy's equation, dimensionless

C = Specific heat of liquid, Btu/lb-°F

G = Mass velocity, $lb/hr\text{-}ft^2$; G' in $lb/sec\text{-}ft^2$

g = Acceleration of gravity

g_c = Conversion factor, 4.17×10^8 $lb_{mass}\text{-}ft/hr^2\text{-}lb_{force}$

h = Nonboiling heat transfer coefficient, $Btu/hr\text{-}ft^2\text{-}°F$

h_{fg} = Latent heat of vaporization, Btu/lb

k = Thermal conductivity of liquid, Btu/hr-ft-°F

K_o = Correlation coefficient in Equation 18, dimensionless

L = Heated channel length, ft

P = Absolute pressure, lb/ft^2, P' in $lb/in.^2$

Pr = Prandtl number, $\left(\frac{C\mu}{k}\right)$, dimensionless

Q = Rate of heat transfer, Btu/hr

Q/A = Heat flux, $Btu/hr\text{-}ft^2$

s = Channel diameter, ft

S = Perimeter of heat transfer area, ft

T = Bulk temperature of liquid, °F

T_s = Saturation temperature, °F

T_w = Surface temperature of heater, °F

v_ℓ = Velocity of liquid, ft/sec

v_g = Velocity of vapor, ft/sec

W = Mass flow rate, lb/hr

x = Vapor quality based on mass flow rate, dimensionless

x^+ = Vapor quality based on mass of fluid present at a given point, dimensionless

α = Void fraction or vapor volume fraction, dimensionless

ΔP_s = Pressure difference corresponding to the superheat ΔT_s, lb/ft^2

ΔT_s = Wall superheat, $(T_w - T)$, °F

ΔT_{sub} = Liquid subcooling, $(T_s - T)$, °F

μ_ℓ = Viscosity of liquid, lb/hr-ft

μ_g = Viscosity of vapor, lb/hr-ft

ρ_ℓ = Density of liquid, lb/ft^3

ρ_g = Density of vapor, lb/ft^3

σ = Surface tension

X = Martinelli parameter defined in text, dimensionless

APPENDIX A
TABLES OF RESULTS

TABLE A-1

ISOPROPYL DIPHENYL BOILING HEAT TRANSFER RESULTS
(Upflow Operation)

Run No.	Mass Velocity (lb/sec-ft^2)	Heat Flux (Btu/hr-ft^2)	Pressure (psia)	T_s-T (°F)	T_w-T_s (°F)
1	430	88,000	33.4	5	43
2	450	80,500	30.3	12	42
3	450	87,000	30.4	6	43
4	450	91,000	30.7	1	44
5	450	95,000	31.8	0	45
6	445	64,000	24.0	17	45
7	440	76,000	24.4	3	48
8	440	84,000	26.7	0	46
9	440	91,500	29.9	0	47
10	540	85,000	22.4	15	52
11	465	83,500	21.8	10	54
12	465	93,000	22.7	0	53
13	540	100,000	22.4	0	54
14	630	84,600	23.2	7	52
15	630	91,400	23.4	3	55
16	630	93,300	24.0	0	53
17	630	96,000	24.6	0	53
18	450	81,000	21.6	15	51
19	360	66,000	22.6	0	49
20	540	95,000	23.2	0	52
21	450	92,600	22.5	10	51
22	630	40,200	22.7	3	41
23	630	44,300	22.9	0	42
24	630	50,700	23.6	0	43
25	425	55,600	25.6	0	42
26	350	45,700	25.7	2	40
27	335	47,500	26.9	5	39
28	405	57,800	26.9	3	41
29	325	48,700	28.1	3	38
30	395	58,000	28.1	5	40
31	380	58,700	29.2	3	40

TABLE A-2

SANTOWAX-R BOILING HEAT TRANSFER

Run No.	Mass Velocity (lb/sec-ft^2)	Heat Flux (Btu/hr-ft^2)	Pressure (psia)	T_s-T (°F)	T_w-T_s (°F)
		(Upflow Operation)			
1	397	87,300	17.9	16	63
2	397	87,300	17.5	16	63
3	397	76,000	16.4	23	63
4	397	86,700	17.3	11	66
5	397	98,300	18.3	2	70
6	388	53,300	16.2	9	56
7	388	65,700	16.7	0	63
8	305	98,700	15.8	0	69
9	305	96,700	18.2	0	65
10	305	108,700	19.3	0	73
11	305	105,000	19.3	0	68
12	296	68,000	15.4	0	64
13	296	76,000	16.3	0	66
14	296	84,400	19.3	0	64
15	296	84,400	20.0	0	64
16	296	84,400	21.0	0	65
17	296	84,400	21.4	0	63
18	296	89,200	22.5	0	68
19	296	94,700	25.3	0	64
20	296	96,800	25.6	0	66
21	296	83,300	23.2	14	58
22	296	90,500	23.0	0	62
23	296	93,200	23.2	0	67
24	296	89,300	25.2	0	60
25	296	101,000	25.6	0	65
26	288	52,300	16.0	0	59
27	288	58,000	20.4	0	55
28	288	64,000	20.8	0	56
29	288	64,000	21.0	0	56
30	288	67,300	21.5	0	58
31	288	71,500	22.0	0	59
32	288	74,100	22.5	0	60
33	288	58,500	23.6	11	56
34	288	64,700	23.2	0	54
35	288	70,700	23.9	0	56
36	487	82,000	17.9	0	69
37	487	92,000	19.5	0	71
38	472	66,700	22.6	2	58
39	472	67,800	23.8	0	57
40	567	67,300	20.4	0	61
41	472	58,200	19.3	0	57
42	472	61,700	20.2	0	55

TABLE A-2 (Continued)

Run No.	Mass Velocity (lb/sec-ft^2)	Heat Flux (Btu/hr-ft^2)	Pressure (psia)	T_s-T (°F)	T_w-T_s (°F)
43	472	64,000	19.2	0	58
44	374	39,900	18.0	0	50
45	374	42,700	18.4	0	50
46	374	43,700	18.5	0	52
47	374	44,000	18.8	0	54
48	374	47,500	19.3	0	55
49	374	38,000	17.6	0	48
50	374	44,500	18.8	0	51
51	288	51,200	22.6	22	49
52	374	37,700	17.6	0	50
53	374	50,000	19.7	0	53
54	374	54,700	21.0	0	57
55	374	56,000	21.3	0	57
56	303	34,300	15.7	57	50
57	303	38,600	16.6	0	52
58	303	38,600	16.6	0	51
59	303	42,100	17.3	0	53
60	303	44,500	17.1	0	52
61	303	45,700	17.0	0	52
62	387	51,300	15.8	5	57
63	387	55,400	16.1	0	57
64	387	58,700	16.5	0	58
65	387	62,800	17.0	0	58
66	468	57,300	20.7	0	55
67	468	60,300	20.9	0	57
68	468	62,700	21.4	0	54
69	296	50,300	15.0	24	55
70	296	57,200	15.6	15	58
71	296	59,700	15.7	7	60
72	296	63,800	15.7	0	61
73	296	70,000	16.0	0	59
74	296	74,600	16.1	0	60
75	315	62,700	17.3	14	59
76	315	66,700	17.7	8	61
77	296	52,800	15.0	21	58
78	296	62,400	15.6	9	52
79	296	66,200	15.6	0	64
80	296	69,000	15.7	0	61
81	315	68,000	16.8	8	63
82	315	74,400	17.1	0	60
83	315	65,300	19.1	20	55
84	296	72,000	19.5	11	59
85	296	76,000	20.3	7	60
86	315	75,400	22.6	20	56
87	315	79,000	23.1	5	65

TABLE A-2 (Continued)

Run No.	Mass Velocity (lb/sec-ft^2)	Heat Flux (Btu/hr-ft^2)	Pressure (psia)	T_s-T (°F)	T_w-T_s (°F)
88	315	83,500	23.5	0	59
89	315	87,000	23.6	0	59
90	387	54,000	16.0	6	58
91	387	65,700	16.7	0	58
92	387	66,400	16.4	0	59
93	387	60,300	16.9	1	59
94	387	67,200	18.1	0	58
95	387	68,800	19.7	12	57
96	387	70,600	20.6	10	56
97	387	76,000	20.5	12	57
98	387	78,000	19.6	0	59
99	482	71,500	17.3	3	64
100	482	79,000	16.7	0	64
101	482	85,000	17.3	0	68
102	482	90,000	16.7	0	65
103	482	92,000	16.7	0	69
104	280	27,900	17.0	0	43
105	280	29,200	17.0	0	43
106	280	31,000	17.3	0	45
107	280	35,000	17.6	0	47
108	280	27,000	19.7	0	42
109	280	34,400	19.5	2	48
110	280	34,000	19.4	0	46
111	280	38,600	19.5	0	47
112	280	34,100	22.6	7	47
113	280	39,000	22.6	0	46
114	280	42,900	22.7	0	47
115	374	37,700	19.6	7	47
116	374	43,700	19.7	0	50
117	374	46,900	19.9	0	51
118	374	43,700	22.6	9	50
119	374	51,000	22.7	0	55
120	374	59,300	22.7	0	52
121	374	61,000	22.8	0	52
122	560	61,000	19.3	0	60
123	560	61,000	20.0	5	53
124	560	68,100	20.3	0	60
125	560	78,300	20.7	0	63
126	560	84,500	22.6	0	62
127	654	80,600	21.4	2	65
128	729	95,000	21.8	0	70
129	468	78,500	22.6	0	58
130	468	86,100	23.4	0	61
131	468	92,500	24.7	0	63
132	468	68,000	19.8	0	58
133	468	78,700	20.5	0	60
134	468	78,700	22.3	0	60

TABLE A-2 (Continued)

Run No.	Mass Velocity (lb/sec-ft^2)	Heat Flux (Btu/hr-ft^2)	Pressure (psia)	T_s-T (°F)	T_w-T_s (°F)
		(Downflow Operation)			
1	468	91,300	25.5	3	62
2	560	67,500	28.3	3	54
3	560	69,000	24.0	8	54
4	560	66,300	24.7	0	59
5	374	48,800	27.6	6	51
6	387	67,400	27.9	10	56
7	387	67,000	27.8	0	57
8	288	46,000	23.7	0	55
9	280	50,000	27.7	6	52
10	387	68,500	24.0	8	59
11	482	90,000	28.0	0	60
12	482	91,300	25.5	8	61
13	387	91,500	27.7	10	59
14	387	68,000	24.0	0	58
15	288	48,300	20.6	9	56
16	280	50,000	28.0	0	50

TABLE A-3

VOID FRACTION RESULTS FOR SUBCOOLED BOILING OF SANTOWAX-R

Run No.	Mass Velocity ($lb/sec-ft^2$)	Pressure (psia)	Heat Flux ($Btu/hr-ft^2$)	T_s-T (°F)	T_w-T (°F)	h ($Btu/hr-ft^2-°F$)	α_{calc}	α_{exp}
			(Upflow Operation)					
1	288	23.5	51,200	22	71	572	0.07	0.05
2	288	24.4	58,500	10	66	572	0.30	0.30
3	468	18.5	43,200	11	49	858	0.01	0.00
4	387	14.9	39,600	12	54	730	0.00	0.00
5	296	15.0	50,300	24	79	590	0.02	0.04
6	296	15.6	57,200	14	73	590	0.14	0.14
7	315	17.3	62,700	12	71	629	0.18	0.16
8	315	17.7	66,700	8	69	629	0.35	0.34
9	296	15.0	52,800	21	79	590	0.04	0.05
10	296	15.6	62,400	9	71	590	0.31	0.30
11	315	16.8	68,000	8	71	629	0.35	0.36
12	315	19.1	65,300	18	73	629	0.13	0.12
13	296	19.5	72,000	10	69	590	0.42	0.40
14	315	22.6	80,000	18	74	629	0.22	0.24
15	315	23.1	79,000	10	68	629	0.43	0.40
16	387	17.4	51,300	16	62	730	0.03	0.09
17	387	19.7	68,800	11	68	730	0.15	0.15
18	387	20.6	70,600	8	65	730	0.26	0.27
19	387	20.5	77,300	11	68	730	0.22	0.31
20	374	22.6	43,700	9	59	716	0.02	0.03
21	654	20.8	69,300	8	60	1,120	0.01	0.03
22	748	20.8	80,000	8	64	1,250	0.00	0.03
23	387	20.5	72,300	10	73	730	0.17	0.20
24	387	20.5	72,300	18	80	730	0.01	0.06
25	296	16.4	51,500	32	80	590	0.02	0.04
26	296	17.0	63,800	18	79	590	0.13	0.12
27	296	19.2	55,300	46	85	590	0.02	0.00
28	294	19.5	55,300	35	82	587	0.05	0.01
29	292	19.7	55,300	25	77	584	0.06	0.02
30	290	19.9	55,300	20	72	580	0.09	0.05
31	288	19.6	55,300	12	67	576	0.19	0.13
32	377	22.5	58,500	34	72	712	0.02	0.01
33	374	22.5	58,500	24	71	709	0.03	0.03
34	371	22.5	58,500	14	66	706	0.08	0.06
35	462	21.9	57,100	52	77	840	0.00	0.00
36	460	21.9	57,100	42	75	837	0.00	0.01
37	458	21.9	57,100	32	73	833	0.00	0.02
38	456	21.9	57,100	22	69	829	0.00	0.03
39	454	21.9	57,100	12	63	826	0.03	0.03
40	280	28.1	43,500	53	72	555	0.01	0.01
41	280	24.7	43,500	39	68	555	0.02	0.03
42	280	21.2	43,500	19	65	555	0.06	0.09
43	296	26.5	82,000	20	82	590	0.23	0.17
44	394	20.2	89,000	18	81	743	0.14	0.13
45	392	20.2	89,000	12	80	740	0.21	0.16

TABLE A-3 (Continued)

Run No.	Mass Velocity (lb/sec-ft^2)	Pressure (psia)	Heat Flux (Btu/hr-ft^2)	T_s-T (°F)	T_w-T (°F)	h (Btu/hr-ft^2-°F)	α_{calc}	α_{exp}
			(Downflow Operation)					
1	315	21.7	70,000	22	74	629	0.13	0.19
2	296	23.7	69,000	18	72	590	0.20	0.18
3	395	23.7	90,000	20	76	740	0.15	0.19
4	296	23.5	70,500	19	71	590	0.20	0.21
5	374	24.1	68,000	13	65	709	0.16	0.14
6	315	23.4	70,000	18	70	629	0.17	0.18
7	387	27.6	71,500	29	70	730	0.06	0.08
8	380	27.6	69,500	22	67	723	0.08	0.12
9	380	27.6	69,000	11	61	723	0.20	0.23
10	395	27.5	95,000	27	78	740	0.12	0.17
11	387	27.5	95,000	13	69	730	0.30	0.29
12	387	27.7	91,500	10	67	730	0.36	0.39
13	482	28.1	92,000	30	80	875	0.05	0.10
14	482	28.2	94,000	19	72	875	0.10	0.13
15	468	28.5	91,500	15	70	858	0.14	0.21
16	482	25.5	92,800	24	84	875	0.05	0.07
17	482	25.5	91,300	19	80	875	0.07	0.12
18	482	25.5	91,300	8	69	875	0.24	0.24
19	288	20.5	52,000	23	77	572	0.05	0.01
20	288	20.6	50,000	15	70	572	0.09	0.05
21	288	20.6	48,300	9	65	572	0.18	0.14
22	482	27.7	90,500	23	81	875	0.05	0.06
23	482	28	90,000	16	76	875	0.09	0.14
24	482	28	89,000	8	68	875	0.23	0.23
25	387	23.7	70,600	22	78	730	0.05	0.05
26	387	24	68,500	16	72	730	0.09	0.09
27	387	24	68,500	8	67	730	0.17	0.21
28	560	27.5	67,500	26	63	1,000	0.01	0.03
29	560	28.1	67,500	19	60	1,000	0.02	0.06
30	560	28.1	67,500	10	60	1,000	0.04	0.08
31	560	23.8	70,500	25	64	1,000	0.01	0.01
32	560	23.8	70,500	13	62	1,000	0.03	0.02
33	560	24	69,000	8	62	1,000	0.04	0.04
34	374	27.4	48,500	22	64	716	0.01	0.03
35	374	27.4	50,500	11	65	716	0.03	0.05
36	387	27.5	68,300	24	69	730	0.07	0.07
37	387	27.8	68,300	17	67	730	0.10	0.12
38	387	27.9	67,400	10	66	730	0.17	0.20
39	288	23.4	46,000	25	75	572	0.02	0.03
40	288	23.7	46,000	20	72	572	0.04	0.05
41	288	23.6	46,000	12	67	572	0.08	0.11
42	280	28.0	50,000	24	69	555	0.08	0.08
43	280	28.1	50,000	15	63	555	0.15	0.12

TABLE A-4

VOID FRACTION RESULTS FOR SUBCOOLED BOILING OF SANTOWAX-R NEAR SATURATION TEMPERATURE

Run No.	Mass Velocity (lb/sec-ft^2)	Pressure (psia)	Heat Flux (Btu/hr-ft^2)	$T_s - T$ (°F)	$T_w - T$ (°F)	h (Btu/hr-ft^2-°F)	α_{calc}	α_{exp}
			(Upflow Operation)					
1	280	16.7	25,100	4	43	555	0.04	0.02
2	280	22.6	34,100	7	53	555	0.12	0.12
3	280	19.5	34,400	2	50	555	0.18	0.16
4	288	15.6	44,200	4	64	572	0.17	0.12
5	288	20.2	54,000	3	68	572	0.31	0.30
6	288	19.5	55,300	1	58	572	0.38	0.35
7	288	19.5	55,300	0	58	572	0.38	0.39
8	288	24.4	58,500	10	66	572	0.37	0.30
9	288	23.2	64,700	0	54	572	0.50	0.57
10	296	15.7	59,700	7	67	590	0.36	0.30
11	296	15.6	62,400	9	71	590	0.36	0.30
12	296	17.7	63,800	0	61	590	0.44	0.43
13	296	15.8	64,000	4	70	590	0.40	0.33
14	296	20.3	76,000	7	67	590	0.44	0.47
15	305	16.6	38,600	0	52	610	0.15	0.16
16	305	16.6	38,600	0	51	610	0.17	0.26
17	305	17.0	44,500	0	52	610	0.26	0.30
18	315	17.7	66,700	8	69	629	0.38	0.34
19	315	16.8	68,000	8	71	629	0.38	0.36
20	315	17.0	72,300	0	58	629	0.49	0.51
21	315	23.1	79,000	10	68	629	0.49	0.40
22	315	23.5	83,500	0	59	629	0.57	0.57
23	346	21.5	41,500	4	48	672	0.18	0.18
24	368	22.5	58,500	4	59	710	0.27	0.19
25	374	16.7	32,100	0	43	716	0.03	0.01
26	374	16.9	33,900	0	46	716	0.02	0.04
27	374	17.0	35,800	0	46	716	0.06	0.05
28	374	19.6	37,700	5	51	716	0.03	0.08
29	374	17.6	37,700	0	50	716	0.04	0.05
30	374	17.6	38,000	0	48	716	0.07	0.10
31	374	18.0	39,900	0	49	716	0.10	0.16
32	374	18.4	42,700	0	50	716	0.13	0.17
33	374	18.5	43,700	0	52	716	0.13	0.18
34	374	22.6	43,700	9	59	716	0.03	0.03
35	374	19.3	47,500	0	51	716	0.20	0.24
36	374	22.7	51,000	0	55	716	0.21	0.25
37	387	15.7	51,300	5	62	730	0.11	0.06
38	387	16.0	54,700	6	64	730	0.15	0.12
39	387	16.1	55,400	0	57	730	0.23	0.19
40	387	16.5	58,700	0	58	730	0.27	0.32
41	387	16.9	60,300	1	59	730	0.27	0.29
42	387	17.0	62,800	0	58	730	0.31	0.35
43	387	17.0	62,800	0	58	730	0.31	0.36
44	387	19.5	64,000	6	67	730	0.24	0.18
45	387	16.7	65,700	0	58	730	0.34	0.35
46	387	16.4	66,400	0	59	730	0.34	0.40
47	387	18.1	67,200	0	58	730	0.36	0.42

TABLE A-4 (Continued)

Run No.	Mass Velocity (lb/sec-ft^2)	Pressure (psia)	Heat Flux (Btu/hr-ft^2)	T_s-T (°F)	T_w-T (°F)	h (Btu/hr-ft^2-°F)	α_{calc}	α_{exp}
48	387	20.6	70,600	8	65	730	0.33	0.27
49	387	20	71,500	5	66	730	0.33	0.38
50	387	20.5	72,300	10	73	730	0.29	0.20
51	387	19.5	73,000	6	67	730	0.34	0.34
52	387	20.0	73,000	3	60	730	0.39	0.42
53	387	19.6	78,000	0	59	730	0.44	0.53
54	387	22.2	86,000	0	57	730	0.50	0.59
55	387	20.2	89,000	3	72	730	0.44	0.33
56	468	18.2	43,200	2	49	858	0.02	0.02
57	468	18.9	48,300	5	54	858	0.04	0.04
58	468	20.7	57,300	0	55	858	0.15	0.10
59	468	19.3	58,300	0	57	858	0.15	0.12
60	468	20.9	60,300	0	57	858	0.17	0.17
61	468	20.2	61,700	0	55	858	0.21	0.18
62	468	21.4	62,700	0	54	858	0.23	0.22
63	468	19.2	64,000	0	58	858	0.21	0.24
64	468	21.7	65,500	0	54	858	0.26	0.25
65	468	19.8	68,000	0	58	858	0.25	0.23
66	468	17.9	82,000	0	69	858	0.29	0.25
67	468	19.5	92,000	0	71	858	0.36	0.32
68	482	17.3	71,500	3	67	875	0.18	0.16
69	482	16.7	79,000	0	64	875	0.29	0.25
70	482	17.3	85,000	0	68	875	0.31	0.32
71	482	16.7	90,000	0	65	875	0.36	0.34
72	482	16.7	92,000	0	69	875	0.36	0.36
73	560	19.3	61,000	0	60	1,000	0.02	0.03
74	560	20.0	61,000	5	58	1,000	0.04	0.08
75	560	20.3	68,100	0	60	1,000	0.11	0.12
76	560	20.7	78,300	0	63	1,000	0.19	0.21
77	560	22.6	84,500	0	62	1,000	0.25	0.25
78	654	20.8	67,200	8	60	1,120	0.03	0.06
79	654	21.4	75,000	2	67	1,120	0.07	0.10
			(Downflow Operation)					
1	280	27.7	50,000	6	58	570	0.33	0.26
2	288	23.7	46,000	0	55	572	0.30	0.28
3	374	27.6	48,800	6	57	716	0.15	0.11
4	374	28.6	50,000	0	48	716	0.26	0.30
5	380	27.6	69,300	4	54	727	0.40	0.46
6	387	27.8	67,000	0	57	730	0.36	0.37
7	387	27.9	67,400	10	66	730	0.29	0.20
8	387	24.0	68,000	0	58	730	0.36	0.37
9	387	24	68,500	8	67	730	0.29	0.17
10	387	27.7	91,500	10	69	730	0.46	0.39
11	468	25.5	91,300	3	65	858	0.39	0.37
12	482	28.0	90,000	0	60	875	0.40	0.46
13	482	25.5	91,300	8	69	875	0.35	0.24
14	560	24.7	66,300	0	59	1,000	0.10	0.13
15	560	28.3	67,500	3	57	1,000	0.14	0.18
16	560	28.1	67,500	10	60	1,000	0.10	0.08
17	560	24.0	69,000	8	62	1,000	0.09	0.04

TABLE A-5

VOID FRACTION RESULTS FOR BULK BOILING OF SANTOWAX-R

Run No.	Mass Velocity ($lb/sec\text{-}ft^2$)	Pressure (psia)	Heat Flux ($Btu/hr\text{-}ft^2$)	Quality (wt%)	X	α	Slip Ratio
			(Upflow Operation)				
1	288	26.5	101,000	8.5	1.11	0.82	2.2
2	288	16.6	52,300	1.4	4.18	0.55	2.4
3	288	20.6	58,000	1.5	4.49	0.58	1.7
4	288	21.4	64,000	6.3	1.27	0.73	3.7
5	288	21.5	64,000	4.0	1.93	0.71	2.5
6	288	22.1	67,300	5.2	1.54	0.74	2.7
7	288	22.6	71,500	6.9	1.20	0.76	3.2
8	288	23.1	74,100	5.2	1.59	0.75	2.4
9	288	24.3	70,700	3.5	2.39	0.70	1.9
10	374	20.8	50,000	0.5	12.0	0.33	1.6
11	374	22.2	54,700	1.4	5.06	0.45	2.5
12	374	22.5	56,000	1.4	5.10	0.45	2.4
13	304	18.1	42,100	1.8	3.45	0.46	4.1
14	304	18.5	44,500	4.0	1.74	0.64	4.2
15	296	16.4	70,000	2.7	2.33	0.68	2.8
16	296	16.9	74,600	5.4	1.24	0.74	4.1
17	296	16.2	69,000	2.2	2.74	0.66	2.2
18	315	17.5	74,400	2.0	3.09	0.58	2.9
19	296	20.6	79,300	2.0	3.50	0.59	2.2
20	280	17.0	27,900	0.5	10.40	0.35	1.9
21	280	17.1	29,200	1.1	5.20	0.42	3.1
22	280	17.7	31,000	2.0	3.13	0.52	3.6
23	280	19.2	35,000	4.5	1.61	0.68	3.8
24	280	20.6	38,600	5.0	1.54	0.68	3.8
25	280	23.1	39,000	1.8	4.16	0.56	1.9
26	280	23.6	42,900	4.3	1.88	0.72	2.3
27	374	20.5	43,700	0.5	11.90	0.30	1.8
28	374	21.4	46,700	0.9	7.31	0.41	1.9
29	374	24.1	59,300	1.8	4.29	0.52	2.1
30	374	24.5	61,000	2.3	3.51	0.55	2.3
31	468	24.7	78,500	1.1	6.78	0.48	1.4
32	468	25.7	86,100	2.2	3.75	0.54	2.2
33	468	27.2	92,500	2.2	3.81	0.59	1.7
34	468	22.5	78,700	0.9	6.77	0.41	1.8
35	468	24.1	78,700	1.3	5.72	0.44	2.1
36	296	16.9	70,600	3.0	2.22	0.61	4.0
37	296	17.7	75,200	7.0	1.00	0.76	4.6
			(Downflow Operation)				
1	263	25.0	66,700	14.0	0.64	0.88	2.6
2	263	24.7	63,300	12.0	0.75	0.80	4.0

TABLE A-5 (Continued)

Run No.	Mass Velocity (lb/sec-ft^2)	Pressure (psia)	Heat Flux (Btu/hr-ft^2)	Quality (wt%)	X	α	Slip Ratio
3	278	25.0	62,900	7.4	1.20	0.72	2.4
4	288	24.6	66,000	8.3	1.07	0.70	4.5
5	288	24.6	67,000	9.2	0.97	0.71	4.8
6	288	24.6	68,000	9.2	0.97	0.72	4.6
7	288	24.6	69,000	11.5	0.78	0.73	5.6
8	288	24.6	70,700	12.0	0.75	0.78	4.5
9	288	24.5	72,200	14.0	0.64	0.80	4.8
10	297	28.7	61,500	1.8	4.8	0.62	1.1
11	297	29.0	64,500	3.7	2.50	0.69	1.7
12	297	28.7	65,200	6.2	1.56	0.71	2.7
13	297	28.7	62,100	6.5	1.46	0.74	2.4
14	297	28.7	69,300	9.7	1.02	0.77	3.1
15	297	28.7	69,300	3.2	2.82	0.64	1.8
16	288	28.7	70,500	6.5	1.46	0.69	3.0
17	288	28.7	73,400	9.7	1.02	0.79	2.8
18	393	24.1	76,000	3.7	2.23	0.67	2.3
19	383	24.1	79,000	6.5	1.30	0.71	3.4
20	393	24.1	84,700	11.0	0.80	0.79	4.0
21	383	24.2	84,000	14.0	0.63	0.88	2.7
22	374	24.2	86,800	17.0	0.52	0.90	2.8
23	383	23.8	73,000	1.8	4.25	0.57	1.7
24	374	23.8	74,700	5.1	1.67	0.69	2.9
25	374	23.7	74,000	5.5	1.54	0.69	3.2
26	383	23.8	75,000	4.8	1.76	0.67	3.0
27	383	23.8	72,700	3.2	2.51	0.70	1.7
28	374	24.0	72,700	3.7	2.23	0.63	1.7
29	364	23.7	74,000	6.5	1.30	0.69	3.8
30	364	23.8	74,500	6.9	1.25	0.69	4.0
31	364	23.9	78,700	5.5	1.67	0.72	2.7
32	364	23.8	67,300	5.5	1.67	0.80	1.8
33	364	24.0	72,000	9.7	0.90	0.83	2.7
34	383	22.1	58,500	0.9	7.5	0.47	1.3
35	383	23.1	62,800	0.9	7.7	0.49	1.2
36	379	23.1	64,000	1.8	4.2	0.51	2.3
37	379	23.3	65,300	1.4	5.2	0.55	1.5
38	379	23.3	65,800	2.3	3.4	0.55	2.5
39	379	24.3	67,000	0.9	7.9	0.47	1.2
40	379	24.3	69,000	1.4	5.3	0.53	1.5
41	379	24.2	70,000	2.3	3.5	0.53	2.5
42	379	24.2	70,700	1.8	4.3	0.56	1.7
43	379	24.3	72,000	1.8	4.3	0.58	1.6
44	379	24.3	73,300	2.3	3.5	0.60	1.9
45	379	24.6	74,800	2.3	3.5	0.59	1.9
46	379	24.8	81,000	3.7	2.3	0.60	3.0
47	379	25.1	79,000	1.4	5.4	0.54	1.4

TABLE A-5 (Continued)

Run No.	Mass Velocity (lb/sec-ft^2)	Pressure (psia)	Heat Flux (Btu/hr-ft^2)	Quality (wt%)	X	α	Slip Ratio
48	379	25.8	89,200	6.0	1.5	0.63	4.1
49	379	26.3	90,500	6.5	1.39	0.63	4.5
50	379	26.9	90,500	4.6	1.98	0.64	2.8
51	379	27.5	98,200	9.2	1.05	0.71	4.2
52	303	24.2	56,600	1.4	5.3	0.57	1.3
53	303	24.2	58,000	1.8	4.3	0.58	1.6
54	303	24.2	59,300	3.7	2.2	0.65	2.5
55	303	24.2	60,700	6.5	1.31	0.72	3.2
56	294	24.3	60,700	8.8	1.01	0.78	3.2
57	303	24.3	62,000	6.9	1.28	0.78	2.5
58	303	23.9	62,000	6.5	1.31	0.78	2.4
59	303	23.9	64,300	9.2	0.95	0.82	2.7
60	303	25.7	64,300	4.1	2.2	0.70	2.0
61	303	25.7	64,300	5.1	1.75	0.78	1.7
62	303	25.7	64,700	5.5	1.63	0.78	1.8
63	303	25.4	66,700	6.5	1.36	0.82	1.7
64	303	25.4	68,000	8.7	1.03	0.82	2.3
65	303	27.6	66,700	3.7	2.5	0.68	1.9
66	303	27.5	69,000	5.5	1.70	0.73	2.2
67	303	27.5	68,000	5.1	1.83	0.75	1.8
68	303	27.2	72,000	9.7	1.00	0.79	3.0
69	303	27.2	72,700	10.0	0.97	0.82	2.6
70	303	27.2	74,000	12.0	0.81	0.84	2.7
71	303	29.3	75,400	9.2	1.08	0.76	3.1
72	303	29.1	76,200	10.0	1.00	0.78	3.1
73	303	29.1	77,700	11.0	0.97	0.82	2.7
74	473	22.5	79,400	1.0	7.0	0.49	1.5
75	473	22.7	81,000	1.0	7.0	0.52	1.2
76	473	22.7	82,700	1.8	4.1	0.53	2.1
77	473	23.6	85,400	1.0	7.2	0.46	1.5
78	473	23.7	86,700	1.4	5.3	0.49	1.8
79	473	23.9	88,700	1.4	5.3	0.52	1.6
80	473	23.9	89,400	1.4	5.3	0.53	1.5
81	473	24.3	90,100	0.9	8.0	0.50	1.1
82	473	24.4	94,000	1.8	4.4	0.54	1.9
83	473	24.5	96,000	2.8	2.9	0.58	2.5
84	473	25.1	101,000	4.1	2.1	0.60	1.7
85	473	24.7	82,600	0.9	8.0	0.42	1.5
86	473	24.8	84,000	0.9	8.0	0.46	1.3
87	473	24.9	84,700	0.9	8.0	0.48	1.2
88	473	25.3	88,700	1.4	5.4	0.50	1.6
89	473	25.5	93,000	2.8	3.0	0.52	3.0
90	473	25.8	97,300	3.7	2.4	0.53	3.7
91	473	26.4	99,000	3.7	2.5	0.55	3.4
92	482	25.8	92,000	2.8	3.0	0.65	1.7
93	482	25.9	95,300	3.7	2.4	0.65	2.3
94	482	26.5	93,300	3.7	2.4	0.65	2.2
95	482	27.1	101,000	6.4	2.0	0.67	3.5

APPENDIX B
METHOD OF ANALYSIS AND PHYSICAL PROPERTIES

The various temperature readings along the test section provided a representative temperature profile of the test section wall and of the flowing coolant. The test section outlet pressure and incremental pressure drop data provided a complete pressure profile of the test section, with allowance for static head changes. This information, coupled with a knowledge of the coolant saturation temperature as a function of pressure, was the basis for evaluation of the data in terms of such basic parameters as wall superheat, coolant subcooling, and quality. The coolant bulk temperature profile also provided a check on the overall accuracy of the power input and flow rate measurements by means of a heat balance for the system.

A typical plot used for the analysis of the Santowax-R data is shown in Figure B-1. It may be observed that, because of the high sensitivity of the saturation temperature even for small pressure changes, the fully developed boiling region of the test section is limited to a relatively small section at the end of the heated section. The heat transfer results presented in this report correspond to this fully developed boiling region. All measurements of void fraction were taken at the end of this region. This represented the highest value of void fraction within the heated length for a specific test. The values of quality, defined as the weight fraction vapor flowing, were determined by extrapolation of the nonboiling coolant bulk temperature line into the boiling region. The difference between the extrapolated nonboiling value of coolant temperature and its actual (saturation) temperature (see Figure B-1) was used to determine quality as follows:

$$x = \frac{(T' - T_s)C}{h_{fg}} \quad .$$

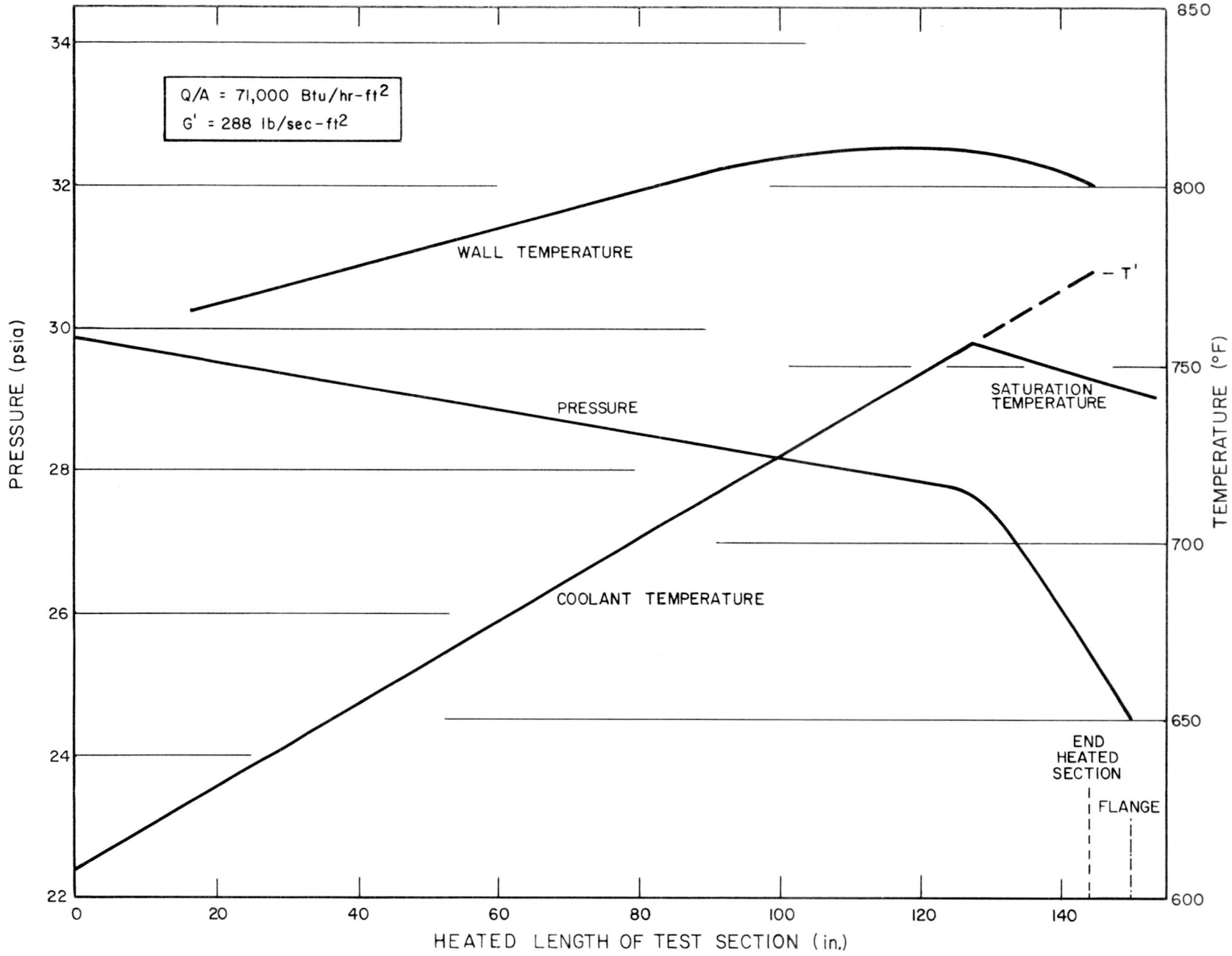

Figure B-1. Typical Steady State Temperature and Pressure Profile in the Test Section

TABLE B-1

PHYSICAL PROPERTIES OF COOLANTS TESTED

ISOPROPYL DIPHENYL*

Temp (°F)	Density (gms/cc)	Viscosity (Centistokes)	Specific Heat (Btu/lb-°F)	Thermal Conductivity (Btu/hr-ft-°F)
300	0.890	0.84	0.512	0.0738
400	0.849	0.55	0.557	0.0713
500	0.808	0.39	0.604	0.0686
600	0.765	0.30	0.649	0.0660

SANTOWAX-R†

Temp (°F)	Density (gms/cc)	Viscosity (Centistokes)	Specific Heat (Btu/lb-°F)	Thermal Conductivity (Btu/hr-ft-°F)
550	0.899	0.44	0.523	0.0673
600	0.876	0.36	0.530	0.0661
650	0.852	0.32	0.536	0.0648
700	0.828	0.28	0.542	0.0636

SATURATION TEMPERATURE

Pressure (psia)	Saturation Temperature (°F)	
	Santowax-R§	Isopropyl Diphenyl*
15	688	557
20	719	582
25	745	600
30	768	616
35	789	630

*See Reference 21.
†See Reference 22.
§Experimentally determined.